

Dopamine Negatively Regulates the NCA Ion Channels in *C. elegans*

Irini Topalidou, Kirsten Cooper[#], and Michael Ailion^{*}

Department of Biochemistry, University of Washington, Seattle, WA, USA

[#]Current address: Fred Hutchinson Cancer Research Center, Seattle, WA, USA

^{*}Corresponding author

Email: mailion@uw.edu (MA)

Short title: NCA regulation by dopamine

16 Abstract

17 The NALCN/NCA ion channel is a cation channel related to voltage-gated sodium and calcium channels.
 18 NALCN has been reported to be a sodium leak channel, but its precise cellular role and regulation are
 19 unclear. We previously found that NCA-1, one of two *Caenorhabditis elegans* orthologs of NALCN, is
 20 activated by a signal transduction pathway acting downstream of the heterotrimeric G protein G_q and the
 21 small GTPase Rho. Using a forward genetic screen, here we identify the GPCR kinase GRK-2 as a new player
 22 in the G_q-Rho-NCA pathway. We find that GRK-2 acts in the head acetylcholine neurons to positively
 23 regulate locomotion and G_q signaling. Using structure-function analysis, we show that the GPCR
 24 phosphorylation and membrane association domains of GRK-2 are required for its function. Our genetic
 25 epistasis data suggest that GRK-2 acts on the D2-like dopamine receptor DOP-3 to inhibit G_o signaling and
 26 positively regulate NCA-1 and NCA-2 activity. We also demonstrate that dopamine, through DOP-3,
 27 negatively regulates NCA-1 and NCA-2 function. Thus, dopamine regulates activity of the NCA channels
 28 through G protein signaling pathways.

29

30 **Author summary**

31 Dopamine is a neurotransmitter that acts in the brain by binding seven transmembrane receptors that
 32 are coupled to heterotrimeric GTP-binding proteins (G proteins). Neuronal G proteins often function by
 33 modulating ion channels that control membrane excitability. Here we identify a molecular cascade
 34 downstream of dopamine in the nematode *C. elegans* that involves activation of the dopamine receptor
 35 DOP-3, activation of the G protein GOA-1, and inactivation of the NCA-1 and NCA-2 ion channels. We also
 36 identify a kinase (GRK-2) that phosphorylates and inactivates the dopamine receptor DOP-3, thus leading
 37 to inactivation of GOA-1 and activation of the NCA channels. Thus, this study connects dopamine signaling
 38 to activity of the NCA channels through G protein signaling pathways.

39

40 Introduction

41 Heterotrimeric G proteins modulate neuronal activity in response to experience or environmental
 42 changes. G_q is one of the four types of heterotrimeric G protein alpha subunits [1] and is a positive
 43 regulator of neuronal activity and synaptic transmission [2–4]. In the canonical G_q pathway, G_q activates
 44 phospholipase Cβ (PLC) to cleave the lipid phosphatidylinositol 4,5-bisphosphate (PIP2) into diacylglycerol
 45 (DAG) and inositol trisphosphate (IP3), which act as second messengers. In a second major G_q signal
 46 transduction pathway, G_q directly binds and activates Rho guanine nucleotide exchange factors (GEFs),
 47 activators of the small GTPase Rho [5–8]. Rho regulates many biological functions including actin
 48 cytoskeleton dynamics and neuronal development, but less is known about Rho function in mature
 49 neurons. In *C. elegans*, Rho has been reported to stimulate synaptic transmission through multiple
 50 pathways [9–11]. We recently identified the NCA-1 channel as a downstream target of a G_q-Rho signaling
 51 pathway in *C. elegans* [12]. We aim to understand the mechanism of activation of this pathway.

52 The NALCN/NCA ion channel is a nonselective cation channel that is a member of the voltage-gated
 53 sodium and calcium channel family [13–15]. The NALCN channel was proposed to be the major contributor
 54 to the sodium leak current that helps set the resting potential of neurons [16], though there is controversy
 55 whether NALCN is indeed a sodium leak channel [17–19]. In humans, mutations in NALCN or its accessory
 56 subunits have been associated with a number of neurological symptoms, including cognitive and
 57 developmental delay [20–33]. In other organisms, mutations in NALCN/NCA or its accessory subunits lead
 58 to defects in rhythmic behaviors [16,34–41].

59 In addition to the G_q-Rho pathway described above, two other mechanisms have been reported to
 60 regulate the activity of the NALCN channel: a G protein-independent activation of NALCN by G protein-
 61 coupled receptors [42,43] and a G protein-dependent regulation by extracellular Ca²⁺ [44]. Here we
 62 identify the G protein-coupled receptor kinase 2, GRK-2, as a positive regulator of the *C. elegans* G_q-Rho-

63 NCA pathway. G protein-coupled receptor kinases (GRKs) are protein kinases that phosphorylate and
 64 desensitize G protein-coupled receptors (GPCRs). In *C. elegans*, *grk-2* is expressed in the nervous system
 65 and required for normal chemosensation [45]. In this study, we show that *C. elegans grk-2* mutants have
 66 locomotion defects due to decreased G_q signaling in head acetylcholine neurons. We find that GRK-2 acts
 67 as a GPCR kinase for the G_o -coupled D2-like dopamine receptor DOP-3 in head acetylcholine neurons. We
 68 further show that inhibition of G_o signaling by GRK-2 leads to activation of the two worm NCA channels
 69 through the G_q -Rho signaling pathway. Finally, we show that dopamine, through activation of DOP-3,
 70 negatively regulates the activity of the NCA channels.

71

Results

The G protein-coupled receptor kinase GRK-2 promotes G_q signaling

To identify regulators of G_q signaling, we performed a forward genetic screen in the nematode *C. elegans* for suppressors of the activated G_q mutant *egl-30(tg26)* [46,47]. The *egl-30(tg26)* mutant is hyperactive and exhibits exaggerated body bends (Fig 1A and B). One of the G_q suppressors (*yak18*) suppresses both the exaggerated body bends and hyperactive locomotion of *egl-30(tg26)* mutants (Fig S1A). When outcrossed away from the *egl-30(tg26)* mutation, *yak-18* mutant animals were shorter than wild type animals, had slow locomotion, and were egg-laying defective (Fig S1B).

We mapped *yak18* to the left arm of Chromosome III and cloned it by whole genome sequencing and a complementation test with the deletion allele *grk-2(gk268)* (Methods). *yak18* is a G to A transition mutation in the W02B3.2 (*grk-2*) ORF that leads to the missense mutation G379E in the kinase domain of GRK-2. GRK-2 is a serine/threonine protein kinase orthologous to the human GPCR kinases GRK2 and GRK3 [45]. The deletion allele *grk-2(gk268)* suppresses activated G_q (Fig 1A and B) and causes identical defects in locomotion, egg-laying, and body-size as *grk-2(yak18)* (Fig 1C, S1C and S1D). We noticed that *grk-2* mutant animals were defective not only in crawling but also in swimming (Fig S2), a locomotion behavior that has distinct kinematics to crawling [48]. Also, *grk-2* mutants restricted their movements to a limited region of a bacterial lawn, whereas wild-type animals explored the entire lawn (Fig S1E).

Our data suggest that GRK-2 regulates locomotion and is a positive regulator of G_q signaling. The standard model of GRK action is that GPCR phosphorylation by GRK triggers GPCR binding to the inhibitory protein arrestin. Arrestin binding to the GPCR blocks GPCR signaling and mediates receptor internalization [49]. We tested whether loss of arrestin causes defects similar to loss of *grk-2* by using a deletion allele in *arr-1*, the only *C. elegans* arrestin homolog. We found that *arr-1(ok401)* mutant animals do not have slow locomotion (Fig S3), suggesting that *C. elegans* arrestin does not regulate locomotion. We were unable to create a double mutant between *arr-1* and *egl-30(tg26)*, suggesting that this double mutant is synthetic

lethal. These differences between *grk-2* and *arr-1* mutants suggest that GRK-2 regulation of locomotion and G_q signaling is independent of arrestin.

In addition to phosphorylation of GPCRs, mammalian GRK2 can also regulate signaling in a phosphorylation-independent manner [50,51]. Thus, we tested whether the kinase activity of GRK-2 is required for proper locomotion and G_q signaling by assaying whether a kinase-dead GRK-2[K220R] mutant [52,53] is capable of rescuing the *grk-2(gk268)* and *egl-30(tg26) grk-2(gk268)* mutants. Wild type GRK-2 restored the locomotion defect of *grk-2(gk268)* mutants (Fig 1C) but the kinase dead GRK-2[K220R] did not rescue either the locomotion defect or the suppression of activated G_q (Fig 1C and D). We conclude that GRK-2 acts as a kinase to regulate locomotion and G_q signaling.

GPCR-phosphorylation and membrane association domains of GRK-2 are required for its function in locomotion

To examine whether GRK-2 acts as a GPCR kinase to control locomotion, we took a structure-function approach (Fig 2A). We took advantage of previously-described mutations that disrupt specific activities of GRK-2, but do not disrupt GRK-2 protein expression or stability [53]. Although GRKs act as kinases for activated GPCRs, mammalian GRKs have been shown to interact with and phosphorylate other molecules as well [50,51]. Therefore although the kinase activity of GRK-2 is required for locomotion, it is possible that GRK-2 is required for phosphorylation of other proteins and not GPCRs. To examine whether phosphorylation of GPCRs is required for GRK-2 function in locomotion, we expressed GRK-2 with mutations (D3K, L4K, V7A/L8A, and D10A) that have been shown to reduce mammalian GRK2 phosphorylation of GPCRs, but that do not affect phosphorylation of other targets [54]. These N-terminal residues of mammalian GRKs form an amphipathic α -helix that contributes specifically to GPCR phosphorylation [55–59]. *grk-2(gk268)* mutants expressing any of these mutant GRK-2 constructs had slow

locomotion like *grk-2(gk268)* (Fig 2B and C), indicating that GPCR phosphorylation is required for GRK-2 function in locomotion *in vivo*.

In mammalian GRKs, interaction of the N-terminal region with the kinase domain (Fig 2A) stabilizes a closed and more active conformation of the enzyme, important for phosphorylation of GPCRs and other substrates [55–57]. Specifically, mutation of mammalian GRK1 Arg191 disrupted phosphorylation of target substrates in addition to GPCRs, suggesting that this residue is critical for conformational changes important for GRK function as a kinase [56]. To determine whether the analogous residue in GRK-2 is required for its function in locomotion, we expressed GRK-2[R195A] in *grk-2(gk268)* mutants. GRK-2[R195A] was not able to rescue the *grk-2(gk268)* locomotion phenotype (Fig 2D), further supporting the model that GRK-2 acts as a GPCR kinase to regulate locomotion.

The RH (Regulator of G protein Signaling Homology) domain of mammalian GRK2 (Fig 2A) does not act in its classical role as an accelerator of the intrinsic GTPase activity of the G_q subunit, but instead interacts with G_q and participates in the uncoupling of GPCRs linked to G_q via a phosphorylation-independent mechanism [51,59]. To examine whether the G_q -binding residues of the RH domain are needed for GRK-2 function in locomotion, we expressed GRK-2[R106A], [Y109I], and [D110A] that correspond to mutations previously shown to disrupt mammalian GRK2 binding to $G_{q/11}$ [60]. All three mutant GRK-2 constructs were able to fully rescue the slow locomotion defect of *grk-2(gk268)* (Fig 2E). These results suggest that GRK-2 binding to G_q (EGL-30) and phosphorylation-independent desensitization of GPCR signaling are not required for GRK-2 function in locomotion.

The pleckstrin homology (PH) domain of mammalian GRK2 (Fig 2A) mediates interactions of GRK2 with membrane phospholipids and $G\beta\gamma$ subunits [51,61–63]. To examine whether phospholipid binding or binding to $G\beta\gamma$ by the PH domain is required for GRK-2 function in locomotion, we expressed GRK-2[K567E] that disrupts phospholipid binding [64] and GRK-2[R587Q] that disrupts binding to $G\beta\gamma$ [64]. Neither of these GRK-2 mutants rescued the locomotion defect of the *grk-2(gk268)* mutant (Fig 2F), suggesting that

both phospholipid and G $\beta\gamma$ binding through the PH domain of GRK-2 are required for GRK-2 function in locomotion.

GRK-2 acts in head acetylcholine neurons to control locomotion

The locomotion phenotype of *grk-2* mutants suggests that it acts in neurons. To determine where GRK-2 acts to control locomotion, we expressed the *grk-2* cDNA under the control of neuronal-specific promoters. Expression of *grk-2* under the pan-neuronal (*Prab-3*) or acetylcholine (*Punc-17*) neuron promoters fully rescued *grk-2(gk268)* mutant locomotion (Fig 3A). Expression in ventral cord acetylcholine motor neurons (*Pacr-2*) did not rescue the locomotion phenotype, but expression driven by an *unc-17* promoter derivative that is expressed mainly in the head acetylcholine neurons (*Punc-17H* [65]) rescued the locomotion phenotype (Fig 3A). Expression of *grk-2* in the premotor command interneurons that express the glutamate receptor *glr-1* (*Pglr-1*) did not restore *grk-2* locomotion (Fig 3A). Finally, to exclude the possibility that the described role of GRK-2 in chemosensation [45] contributes to the slow locomotion phenotype of *grk-2* mutants, we expressed *grk-2* under ciliated sensory neuron promoters (*Pxbx-1* and *Posm-6*). Expression of *grk-2* in ciliated sensory neurons did not rescue the slow locomotion of *grk-2* mutants (Fig 3A). We conclude that *grk-2* acts in head acetylcholine neurons to regulate locomotion.

To determine if *grk-2* also acts in head acetylcholine neurons to regulate G $_q$ signaling, we expressed *grk-2* cDNA in the head acetylcholine neurons of *egl-30(tg26)* *grk-2* double mutants. Expression in head acetylcholine neurons rescues the *grk-2* suppression of the deep body bends and hyperactive locomotion of activated G $_q$ (Fig 3B and C). These results suggest that *grk-2* acts in head acetylcholine neurons to positively regulate G $_q$ signaling.

GRK-2 is broadly expressed in body and head neurons [45]. To determine if *grk-2* is expressed in head acetylcholine neurons, we coexpressed tagRFP fused to GRK-2 under the *grk-2* promoter (*grk-2::tagRFP*) and GFP under a head acetylcholine neuron promoter (*Punc-17H::GFP*). We observed that *grk-2::tagRFP* is

expressed broadly in head neurons and colocalizes with GFP in at least eight head acetylcholine neurons (Fig 3D). We conclude that GRK-2 is expressed in head acetylcholine neurons to regulate locomotion and G_q signaling.

GRK-2 acts upstream of G_o to regulate locomotion

We have shown that GRK-2 acts as a GPCR kinase to regulate locomotion. If GRK-2 were a kinase for a GPCR coupled to G_q (EGL-30 in *C. elegans*) then we would expect GRK-2 to negatively regulate G_q , which does not agree with our data. Alternatively, GRK-2 could be a kinase for a GPCR coupled to G_o (GOA-1 in *C. elegans*). The *C. elegans* G_q and G_o pathways act in opposite ways to regulate locomotion by controlling acetylcholine release [66]. EGL-30 is a positive regulator of acetylcholine release whereas GOA-1 negatively regulates the EGL-30 pathway through activation of the RGS protein EAT-16 and the diacylglycerol kinase DGK-1. *egl-30* loss-of-function mutants are immobile whereas *egl-30* gain-of-function mutants are hyperactive and have exaggerated body bends [67,68]. *goa-1* mutants have locomotion phenotypes opposite those of *egl-30*. Specifically, *goa-1* loss-of function mutants are hyperactive and have exaggerated body bends [69,70]. Similar to *goa-1* loss-of-function mutants, *eat-16* and *dgk-1* loss-of-function mutants are also hyperactive [71,72]. To test whether GRK-2 acts on a G_o -coupled GPCR, we examined whether *grk-2* mutations suppress the hyperactive phenotype of *goa-1* mutants. The *grk-2 goa-1* double mutant is hyperactive like the *goa-1* single mutant (Fig S4A), indicating that GRK-2 acts upstream of *goa-1*. This result suggests that GRK-2 acts on GPCR(s) coupled to G_o .

To further dissect the GRK-2 pathway, we examined whether *grk-2* mutations suppress the hyperactive phenotypes of *eat-16* and *dgk-1* mutants. The *grk-2 eat-16* double mutant is hyperactive like the *eat-16* single mutant (Fig S4A), indicating that *eat-16*, like *goa-1*, acts downstream of GRK-2. By contrast, the *grk-2 dgk-1* double mutant is similar to *grk-2* (Fig S4B). Expression of the kinase dead GRK-2[K220R] in *grk-2 dgk-1* mutants does not restore *dgk-1* hyperactive locomotion (Fig S4C), indicating that this GRK-2 function

requires its kinase activity, like its roles in regulating locomotion and G_q signaling. In addition, expression of GRK-2 under a head acetylcholine neuron promoter in *grk-2 dgk-1* mutants restores *dgk-1* hyperactive locomotion (Fig S4D), consistent with our data showing that GRK-2 functions in head acetylcholine neurons to control locomotion. The strong suppression of *dgk-1* hyperactivity by a *grk-2* mutation suggests that GRK-2 affects a process that is downstream of DGK-1 action or in parallel to it.

GRK-2 regulates the DOP-3 dopamine receptor

A potential GPCR target for GRK-2 is the G_o -coupled D2-like dopamine receptor DOP-3. In *C. elegans*, dopamine is required for the “basal slowing response”, a behavior in which wild type animals slow down when on a bacterial lawn [73]. This behavior is mediated by mechanosensory activation of the dopamine neurons. *cat-2* mutants that are deficient in dopamine biosynthesis [74] or *dop-3* mutants that lack the D2-like dopamine receptor DOP-3, are defective in basal slowing [73,75]. DOP-3 has been proposed to act through G_o in ventral cord acetylcholine motor neurons to decrease acetylcholine release and promote the basal slowing response [75].

If *grk-2* acts in the dopamine pathway to mediate proper locomotion, possibly by phosphorylating and inactivating DOP-3, then mutations in *dop-3* and *cat-2* should suppress the *grk-2* locomotion phenotype. The *grk-2* mutant slow locomotion phenotype was fully suppressed by a *dop-3* mutation and partially suppressed by a *cat-2* mutation (Fig 4A). A *dop-3* mutation also suppressed the swimming defect of *grk-2* mutants (Fig S2). In addition, *dop-3* and *cat-2* mutations suppressed the *grk-2* suppression of the deep body bends and hyperactive locomotion of activated G_q – that is, the triple mutants resemble the activated G_q single mutant (Fig 4B-E). These results suggest that GRK-2 acts in the dopamine pathway for locomotion and G_q signaling, by negatively regulating the D2-like dopamine receptor DOP-3.

We have shown that GRK-2 acts in head acetylcholine neurons to regulate locomotion. To test if DOP-3 acts in the same neurons as GRK-2 to regulate GRK-2-dependent locomotion, we expressed the *dop-3*

cDNA under a pan-neuronal promoter (*Prab-3*), an acetylcholine neuron promoter (*Punc-17*), a head acetylcholine neuron promoter (*Punc-17H*) and an acetylcholine motor neuron promoter (*Pacr-2*) in the *grk-2 dop-3* double mutant. Expression driven by the pan-neuronal, acetylcholine neuron, and head acetylcholine neuron promoters rescued the *dop-3* suppression of the slow locomotion of *grk-2(gk268)* mutant animals (Fig S5A). We conclude that *dop-3*, like *grk-2*, acts in head acetylcholine neurons to mediate the effects of GRK-2 on locomotion, consistent with the model that GRK-2 acts directly on DOP-3.

We observed that *grk-2 dop-3* and *grk-2 cat-2* double mutant animals still retain some of the characteristic *grk-2* phenotypes: the animals have shorter bodies and are egg-laying defective. In addition, *grk-2* mutants do not fully explore a bacterial lawn and this behavior remains in the *grk-2 dop-3* double mutant (Fig S1E). We suggest that GRK-2 has additional neuronal functions that do not depend on *dop-3*.

The D1-like dopamine receptor DOP-1 has been shown to act antagonistically to DOP-3 to regulate the basal slowing response: *dop-1* mutations suppress the *dop-3* basal slowing phenotype [75]. By contrast, we found that DOP-1 is not involved in the GRK-2 and DOP-3 pathway in locomotion because *dop-1* mutations do not affect the locomotion of *grk-2 dop-3* double mutants (Fig S5B). Thus, the role of DOP-3 in GRK-2-regulated locomotion is independent of its role in the basal slowing response.

Exposure of *C. elegans* to exogenous dopamine causes paralysis in a manner highly dependent on *dop-3* as *dop-3* mutants are significantly resistant to the paralytic effects of exogenous dopamine [75]. If GRK-2 negatively regulates DOP-3, then *grk-2* mutants might be hypersensitive to dopamine due to increased DOP-3 activity. Indeed, we found that *grk-2* mutants are hypersensitive to dopamine and this hypersensitivity depends on *dop-3* (Fig 4F).

GRK-2 is a positive regulator of NCA-1 and NCA-2 channel activity

In addition to the canonical G_q pathway, our screen for suppressors of activated G_q also identified the Trio RhoGEF (UNC-73 in *C. elegans*) as a new direct G_q effector [8]. Recently, we identified the cation

channel NCA-1 as a downstream target of this G_q -Rho pathway [12]. To examine whether *grk-2* acts in the Rho-NCA pathway, we built double mutants of *grk-2* with an activated Rho mutant (G14V), referred to here as Rho*, expressed in acetylcholine neurons. Rho* has an exaggerated waveform and slow locomotion (Fig S6A and B). *grk-2* mutants partially suppress the deep body bends and slow locomotion of Rho*, suggesting that *grk-2* acts downstream of or in parallel to Rho (Fig S6A and B). We also built double mutants of *grk-2* and a dominant activating mutation in the NCA-1 channel gene, *nca-1(ox352)*, referred to here as Nca* [24]. Like Rho*, Nca* mutants have an exaggerated waveform and slow locomotion, but *grk-2* mutants do not suppress either of these phenotypes (Fig S6C and D).

C. elegans has two proteins that encode pore-forming subunits of NCA channels, NCA-1 and NCA-2. Mutations that disrupt both NCA-1 and NCA-2 channel activity cause a characteristic “fainter” phenotype in which worms suddenly arrest their locomotion [35]. Our genetic experiments indicate that GRK-2 acts in the Rho-NCA pathway, but *grk-2* mutants are not fainters. Given that *grk-2* partially suppresses Rho*, we hypothesized that GRK-2 is not absolutely required in the Rho-NCA pathway, but provides modulatory input. To test this hypothesis we built double mutants between *grk-2* and *nlf-1*, which is partially required for localization of the NCA-1 and NCA-2 channels and has a weak fainter mutant phenotype [12,76]. A *grk-2* mutation strongly enhanced the weak fainter phenotype of an *nlf-1* mutant so that the double mutants resembled the stronger fainter mutants that completely abolish NCA-1 and NCA-2 channel activity (Fig 5A and B). Moreover, double mutants between *grk-2* and the RhoGEF Trio *unc-73* were also strong fainters, supporting the hypothesis that GRK-2 acts in the Rho-NCA pathway (Fig 5C). By contrast, double mutants between *grk-2* and the PLC *egl-8* do not have a fainter phenotype (Fig 5C). These results suggest that GRK-2 is a positive regulator of NCA-1 and NCA-2 channel activity.

If GRK-2 regulates the NCA channels by acting as a negative regulator of G_o then we would expect that mutations in other proteins that act as negative regulators of G_o would enhance the fainter phenotype of *nlf-1* mutants. Indeed, a mutant in EGL-10, the G_o RGS that negatively regulates G_o [77], strongly enhances

the *nlf-1* fainter phenotype (Fig 5D). As controls, mutations in genes involved in dense-core vesicle biogenesis (*eipr-1* and *cccp-1*) that cause locomotion defects comparable to *grk-2* or *egl-10* [47,65] did not enhance the *nlf-1* fainter phenotype, indicating that these are specific interactions of *grk-2* and *egl-10* with *nlf-1*.

Because *grk-2* and *nlf-1* act in head acetylcholine neurons to mediate locomotion [12], we predicted that expression of an activated GOA-1 mutant under a head acetylcholine neuron promoter would enhance the fainter phenotype of *nlf-1* mutants. Indeed, we found that expression of the activated G_o mutant GOA-1[Q205L] in head acetylcholine neurons makes the animals slow (Fig 5E) and significantly enhances the fainter phenotype of *nlf-1* mutants (Fig 5F). These results support the model that GRK-2 negatively regulates G_o and that G_o negatively regulates NCA-1 and NCA-2 channel activity.

Dopamine acts through DOP-3 to negatively regulate NCA-1 and NCA-2 channel activity

Our results show that GRK-2 acts in locomotion by negatively regulating DOP-3, and that GRK-2 is a positive regulator of NCA-1 and NCA-2 activity. These data predict that DOP-3 would be a negative regulator of NCA-1 and NCA-2 channel activity. Consistent with this model, mutations in *dop-3* and *cat-2* almost fully suppress the *nlf-1* fainter phenotype during forward movement (Fig 6A and B). Moreover, *dop-3* mutants partially suppress the strong *grk-2 nlf-1* fainter phenotype, consistent with the model that DOP-3 is a GPCR for GRK-2 (Fig 6C). These results suggest that dopamine, through DOP-3, negatively regulates NCA-1 and NCA-2 channel activity.

Our model suggests that GRK-2 and DOP-3 play modulatory and not essential roles in the regulation of NCA-1 and NCA-2 channel activity. By contrast, UNC-80 is necessary for the stability and function of NCA-1 and NCA-2, so *unc-80* mutants are strong fainters [36,39]. As expected for a modulatory role in regulating NCA-1 and NCA-2 activity, mutations in *dop-3* and *cat-2* do not suppress the strong fainter phenotype of *unc-80* mutants (Fig S7A and S7B).

We showed above that *grk-2* mutants are hypersensitive to the paralytic effects of dopamine. We also found that low concentrations of dopamine do not paralyze *grk-2* mutants and instead cause them to faint, and that this effect depends on *dop-3* (Fig 6D). This is consistent with the model that dopamine acts through DOP-3 to negatively regulate NCA-1 and NCA-2.

Discussion

In this study we identified a pathway that regulates the activity of the NCA-1 and NCA-2 channels through dopamine and G_q signaling (Fig 7). We found that dopamine acts through the D2-like receptor DOP-3 to negatively regulate NCA-1 and NCA-2. Furthermore, we identified the GPCR kinase GRK-2 as a positive regulator of G_q and negative regulator of NCA-1 and NCA-2. Our results suggest that GRK-2 mediates its regulatory effects by inhibiting DOP-3.

C. elegans GRK-2 was previously shown to act in sensory neurons to regulate chemosensation [45]. Our data show that GRK-2 acts in head acetylcholine neurons to regulate locomotion and G_q signaling. In both chemosensation and locomotion, GRK-2 acts as a GPCR kinase and membrane localization is critical for its function [53]. Additionally, GRK-2 acts independently of arrestin to regulate both these behaviors [45]. Because *cat-2* and *dop-3* mutants are hypersensitive to the aversive odorant octanol [78–80] and *grk-2* mutants are insensitive to octanol [45], GRK-2 might act as a GPCR kinase for DOP-3 in chemosensory neurons as well.

The D2-type dopamine receptors, like DOP-3, are GPCRs that couple to members of the inhibitory G_{i/o} family. Mammalian GRK2 and GRK3 (the orthologs of GRK-2) have been connected to the desensitization, internalization, and recycling of D2-type dopamine receptors [81–86]. Interestingly, it is possible that at least some of the effects of GRK2 on D2 receptor function may be independent of receptor phosphorylation [81,85,86], though one caveat of these studies is that they involve GRK2 overexpression in heterologous cells. *In vivo* studies of the role of mammalian GRKs in the regulation of dopamine receptors have focused on the analysis of behaviors that are induced by psychostimulatory drugs such as cocaine that elevate the extracellular concentration of dopamine [82]. Mice with a cell-specific knockout of GRK2 in D2 receptor-expressing neurons have altered spontaneous locomotion and sensitivity to cocaine [87], though the cellular mechanisms underlying these behavioral effects are not known. Our findings

provide evidence of a direct association between GRK-2 and D2-type receptor signaling that regulates locomotion in an *in vivo* system.

grk-2 is a partial suppressor of activated Rho, suggesting that *grk-2* modulates activity of the G_q-Rho signaling pathway which acts in parallel to the canonical G_q pathway [5–8]. In *C. elegans*, Rho acts as a presynaptic activator of neurotransmitter release in part through inhibition of diacylglycerol kinase (DGK-1) and accumulation of presynaptic DAG [11]. Thus, inhibition of G_o by GRK-2 could promote G_q-Rho signaling by two mechanisms: (1) by inhibiting the G_q RGS EAT-16 and thus activating G_q itself, and (2) by inhibiting DGK-1 which acts in parallel to G_q-Rho to regulate DAG levels (Fig 7). Interestingly, a *grk-2* mutant is suppressed by mutations in *goa-1* and *eat-16*, but not by *dgk-1*. These findings add to other literature showing that *goa-1* and *eat-16* have similar interactions with G_q signaling, but that *dgk-1* is distinct [71,88].

Recently we showed that the G_q-Rho signaling pathway positively regulates NCA-1 channel function [12]. In *C. elegans*, the NCA-1 and NCA-2 channels mediate persistent motor circuit activity and sustained locomotion [89]. The identification of GRK-2 as a DOP-3 kinase and positive regulator of G_q-Rho signaling connect dopamine signaling to regulation of the NCA channels (Fig 7). We showed that GRK-2, DOP-3, and GOA-1 all act in head acetylcholine neurons to regulate locomotion, and the NCA channels have also been shown to act in head acetylcholine neurons [12]. Thus, we propose that dopamine signaling through DOP-3 and G_o activation may act cell autonomously to inhibit NCA-1 and NCA-2 activity.

335 **Methods**

336 **Strains**

337 Strains were maintained at room temperature or 20° on the OP50 strain of *E. coli* [90].

338 The Supplementary Information contains full genotypes of all the strains we used (S1 Table; List of strains).

339

340 **Isolation and identification of the *grk-2(yak18)* mutation**

341 The *grk-2(yak18)* mutant was isolated in an ENU screen as a suppressor of the hyperactive locomotion
342 and deep body bends of the activated G_q mutant *egl-30(tg26)* [47]. We mapped the *yak18* mutation to the
343 left arm of Chromosome III (between -27 and -21.8 m.u.) using a PCR mapping strategy that takes
344 advantage of PCR length polymorphisms due to indels in the Hawaiian strain CB4856 (Jihong Bai,
345 unpublished data). Using whole-genome sequencing (see below), we found that *yak18* is a G to A
346 transition mutation in the W02B3.2 (*grk-2*) ORF that creates a G379E missense mutation in the kinase
347 domain of GRK-2. We confirmed the gene identification by performing a complementation test with the
348 *grk-2(gk268)* deletion mutant.

349

350 **Whole-Genome Sequencing**

351 Genomic DNA was isolated and purified according to the Worm Genomic DNA prep protocol from the
352 Hobert lab website (http://hobertlab.org/wp-content/uploads/2013/02/Worm_Genomic_DNA_Prep.pdf).
353 The sample was sequenced using Ion Torrent sequencing (DNA Sequencing Core Facility, University of
354 Utah) and the resulting data were analyzed using CloudMap on the Galaxy platform [91].

355

356 **Constructs and transgenes**

357 The Supplemental Information contains a complete list of constructs used (S2 Table; List of plasmids).
358 All constructs made in this study were constructed using the multisite Gateway system from Invitrogen.

Specifically, a promoter region, a gene region (cDNA), and an N- or C-terminal 3'UTR or fluorescent tag (GFP or tagRFP) fused to a 3'UTR were cloned into the destination vector pCFJ150 [92]. For the cell-specific rescuing experiments, an operon GFP was included in the expression constructs downstream of the 3'UTR [93]. This resulted in expression of untagged *grk-2*, *dop-3*, or *goa-1*, but allowed for confirmation of proper promoter expression by monitoring GFP expression.

Extrachromosomal arrays were made by standard injection and transformation methods [94]. In all cases we injected 5-10 ng/ul of the expression vector and isolated multiple independent lines. At least two lines were tested that behaved similarly.

Expression of *grk-2*

We made constructs driving expression of *grk-2* cDNA fused to GFP or tagRFP under the *grk-2* promoter and generated worms with extrachromosomal arrays. For the *grk-2* promoter region, we PCR amplified 2892 bp upstream of the start codon using genomic DNA as a template and the following set of primers: forward primer 5'cagcacagtttccatagtgattgg3' and reverse primer 5'tttttgttctgcaaaatcgaattg3'. *grk-2* showed expression in neurons in the head, ventral cord, and tail, consistent with the published expression pattern [45].

Locomotion and egg-laying assays

For most experiments, we measured locomotion using the body bend assay. Specifically, first-day adults were picked to a three-day-old lawn of OP50 and stimulated by poking the tail of the animal with a worm pick. Body bends were counted for one minute. A body bend was defined as the movement of the worm from maximum to minimum amplitude of the sine wave [88]. Specifically for the experiment described in Fig S6D we used the radial locomotion assay. Animals were placed in the center of 10 cm

plates with thin one to two-day-old lawns of OP50 and left for one hour. The position of each worm was marked and the radial distance from the center of the plate was measured (cm travelled/h).

Egg-laying assays were performed as described [65]. L4 larvae were placed on plates with OP50 at 25°C overnight. The next day, five animals were moved to a fresh plate and allowed to lay eggs at 25°C for two hours. The number of eggs present on the plate was counted.

Fainting assays

First-day adults were transferred to plates with two to three-day-old lawns of OP50 and left undisturbed for one minute. Animals were then poked either on the head (for backward movement) or on the tail (for forward movement), and we counted the number of body bends before the animal faints. If the animal made ten body bends, the assay was stopped and we recorded ten as the number. Thus, animals that never faint (for example, wild-type) are scored as 10 in these experiments. Specifically for the experiment described in Fig 6D the number reported was the percentage of animals that fainted before making 10 body bends.

Swimming assays

Single, first-day adults were transferred to 25 ul of M9 at the center of an empty NGM plate and video recorded for 30 sec. The swimming behavior was analyzed as described [38,48].

Body length measurements

First-day adults were mounted on 2% agarose pads and anesthetized in M9 buffer containing 50 mM sodium azide for ten minutes. The image of each animal was obtained using a Nikon 80i wide-field compound microscope. Body size was measured using ImageJ software.

Dopamine resistance assays

We used a method similar to the one described [75]. Specifically, first-day adults were transferred to plates containing dopamine (2 mM, 5 mM, 10 mM, 15 mM, 20 mM, 40 mM) and incubated for 20 min at room temperature. Animals were then poked using a worm-pick and the number of body bends was counted, stopping the assay at 10 body bends. We report the percent of animals that moved 10 body bends without stopping (Percent of animals moving). A body bend was defined as the movement of the worm from maximum to minimum amplitude of the sine wave. Dopamine plates were prepared fresh just before use, as described [75].

Imaging

For fluorescence imaging, first-day adult animals were mounted on 2% agarose pads and anesthetized with 50 mM sodium azide for ten minutes before placing the cover slip. Images were obtained using an Olympus confocal microscope.

For pictures of worms, first-day adult animals were placed on an assay plate and photographed at 50 or 60X using a Nikon SMZ18 dissecting microscope with a DS-L3 camera control system. The images were processed using ImageJ.

Statistics

P values were determined using GraphPad Prism 5.0d (GraphPad Software). Normally distributed data sets requiring multiple comparisons were analyzed by a one-way ANOVA followed by a Bonferroni or Dunnett test. Normally distributed pairwise data comparisons were analyzed by two-tailed unpaired t tests. Non-normally distributed data sets with multiple comparisons were analyzed by a Kruskal-Wallis nonparametric ANOVA followed by Dunn's test to examine selected comparisons. Non-normally distributed pairwise data comparisons were analyzed by a Mann-Whitney test.

430

431 **Acknowledgments**

432 Special thanks to Denise Ferkey and Jordan Wood for generously providing the *grk-2* mutant
 433 constructs, Jihong Bai for discussions and sharing unpublished methods and equipment, Yongming Dong
 434 for help with the swimming assay, Jill Hoyt for making the *grk-2 nlf-1* double mutant, Jill Hoyt and Jordan
 435 Hoyt for help with the analysis of the whole-genome sequencing data, Dana Miller for sharing equipment,
 436 and the Kraemer lab for insightful ideas. Some strains were provided by the CGC, which is funded by the
 437 NIH Office of Research Infrastructure Programs (P40 OD010440).

438

References

1. Wilkie TM, Gilbert DJ, Olsen AS, Chen XN, Amatruda TT, Korenberg JR, et al. Evolution of the mammalian G protein alpha subunit multigene family. *Nat Genet.* 1992;1: 85–91. doi:10.1038/ng0592-85
2. Coulon P, Kanyshkova T, Broicher T, Munsch T, Wettschureck N, Seidenbecher T, et al. Activity Modes in Thalamocortical Relay Neurons are Modulated by G(q)/G(11) Family G-proteins - Serotonergic and Glutamatergic Signaling. *Front Cell Neurosci.* 2010;4: 132. doi:10.3389/fncel.2010.00132
3. Gamper N, Reznikov V, Yamada Y, Yang J, Shapiro MS. Phosphatidylinositol 4,5-bisphosphate signals underlie receptor-specific Gq/11-mediated modulation of N-type Ca²⁺ channels. *J Neurosci.* 2004;24: 10980–10992. doi:10.1523/JNEUROSCI.3869-04.2004
4. Krause M, Offermanns S, Stocker M, Pedarzani P. Functional specificity of G alpha q and G alpha 11 in the cholinergic and glutamatergic modulation of potassium currents and excitability in hippocampal neurons. *J Neurosci.* 2002;22: 666–673.
5. Lutz S, Freichel-Blomquist A, Yang Y, Rümenapp U, Jakobs KH, Schmidt M, et al. The guanine nucleotide exchange factor p63RhoGEF, a specific link between Gq/11-coupled receptor signaling and RhoA. *J Biol Chem.* 2005;280: 11134–11139. doi:10.1074/jbc.M411322200
6. Lutz S, Shankaranarayanan A, Coco C, Ridilla M, Nance MR, Vettel C, et al. Structure of Galphaq-p63RhoGEF-RhoA complex reveals a pathway for the activation of RhoA by GPCRs. *Science.* 2007;318: 1923–1927. doi:10.1126/science.1147554

- 459 7. Rojas RJ, Yohe ME, Gershburg S, Kawano T, Kozasa T, Sondek J. Galphaq directly activates
460 p63RhoGEF and Trio via a conserved extension of the Dbl homology-associated pleckstrin
461 homology domain. J Biol Chem. 2007;282: 29201–29210. doi:10.1074/jbc.M703458200

- 462 8. Williams SL, Lutz S, Charlie NK, Vettel C, Ailion M, Coco C, et al. Trio’s Rho-specific GEF domain is
463 the missing Galpha q effector in C. elegans. Genes Dev. 2007;21: 2731–2746.
464 doi:10.1101/gad.1592007

- 465 9. Chan JP, Hu Z, Sieburth D. Recruitment of sphingosine kinase to presynaptic terminals by a
466 conserved muscarinic signaling pathway promotes neurotransmitter release. Genes Dev.
467 2012;26: 1070–1085. doi:10.1101/gad.188003.112

- 468 10. Hiley E, McMullan R, Nurrish SJ. The Galpha12-RGS RhoGEF-RhoA signalling pathway regulates
469 neurotransmitter release in C. elegans. EMBO J. 2006;25: 5884–5895.
470 doi:10.1038/sj.emboj.7601458

- 471 11. McMullan R, Hiley E, Morrison P, Nurrish SJ. Rho is a presynaptic activator of neurotransmitter
472 release at pre-existing synapses in C. elegans. Genes Dev. 2006;20: 65–76.
473 doi:10.1101/gad.359706

- 474 12. Topalidou I, Chen P-A, Cooper K, Watanabe S, Jorgensen EM, Ailion M. The NCA-1 ion channel
475 functions downstream of Gq and Rho to regulate locomotion in C. elegans. bioRxiv. 2016;
476 doi:10.1101/090514

- 477 13. Ren D. Sodium leak channels in neuronal excitability and rhythmic behaviors. Neuron. 2011;72:
478 899–911. doi:10.1016/j.neuron.2011.12.007

- 479 14. Liebeskind BJ, Hillis DM, Zakon HH. Phylogeny unites animal sodium leak channels with fungal
480 calcium channels in an ancient, voltage-insensitive clade. *Mol Biol Evol.* 2012;29: 3613–3616.
481 doi:10.1093/molbev/mss182
- 482 15. Lee JH, Cribbs LL, Perez-Reyes E. Cloning of a novel four repeat protein related to voltage-gated
483 sodium and calcium channels. *FEBS Lett.* 1999;445: 231–236.
- 484 16. Lu B, Su Y, Das S, Liu J, Xia J, Ren D. The neuronal channel NALCN contributes resting sodium
485 permeability and is required for normal respiratory rhythm. *Cell.* 2007;129: 371–383.
486 doi:10.1016/j.cell.2007.02.041
- 487 17. Boone AN, Senatore A, Chemin J, Monteil A, Spafford JD. Gd³⁺ and calcium sensitive, sodium leak
488 currents are features of weak membrane-glass seals in patch clamp recordings. *PloS One.* 2014;9:
489 e98808. doi:10.1371/journal.pone.0098808
- 490 18. Senatore A, Spafford JD. A uniquely adaptable pore is consistent with NALCN being an ion sensor.
491 *Channels.* 2013;7: 60–68. doi:10.4161/chan.23981
- 492 19. Senatore A, Monteil A, van Minnen J, Smit AB, Spafford JD. NALCN ion channels have alternative
493 selectivity filters resembling calcium channels or sodium channels. *PloS One.* 2013;8: e55088.
494 doi:10.1371/journal.pone.0055088
- 495 20. Al-Sayed MD, Al-Zaidan H, Albakheet A, Hakami H, Kenana R, Al-Yafee Y, et al. Mutations in
496 NALCN cause an autosomal-recessive syndrome with severe hypotonia, speech impairment, and
497 cognitive delay. *Am J Hum Genet.* 2013;93: 721–726. doi:10.1016/j.ajhg.2013.08.001
- 498 21. Chong JX, McMillin MJ, Shively KM, Beck AE, Marvin CT, Armenteros JR, et al. De novo mutations
499 in NALCN cause a syndrome characterized by congenital contractures of the limbs and face,

hypotonia, and developmental delay. Am J Hum Genet. 2015;96: 462–473.
doi:10.1016/j.ajhg.2015.01.003

22. Fukai R, Saitsu H, Okamoto N, Sakai Y, Fattal-Valevski A, Masaaki S, et al. De novo missense mutations in NALCN cause developmental and intellectual impairment with hypotonia. J Hum Genet. 2016;61: 451–455. doi:10.1038/jhg.2015.163

23. Aoyagi K, Rossignol E, Hamdan FF, Mulcahy B, Xie L, Nagamatsu S, et al. A Gain-of-Function Mutation in NALCN in a Child with Intellectual Disability, Ataxia, and Arthrogryposis. Hum Mutat. 2015;36: 753–757. doi:10.1002/humu.22797

24. Bend EG, Si Y, Stevenson DA, Bayrak-Toydemir P, Newcomb TM, Jorgensen EM, et al. NALCN channelopathies: Distinguishing gain-of-function and loss-of-function mutations. Neurology. 2016;87: 1131–1139. doi:10.1212/WNL.0000000000003095

25. Gal M, Magen D, Zahran Y, Ravid S, Eran A, Khayat M, et al. A novel homozygous splice site mutation in NALCN identified in siblings with cachexia, strabismus, severe intellectual disability, epilepsy and abnormal respiratory rhythm. Eur J Med Genet. 2016;59: 204–209. doi:10.1016/j.ejmg.2016.02.007

26. Karakaya M, Heller R, Kunde V, Zimmer K-P, Chao C-M, Nürnberg P, et al. Novel Mutations in the Nonselective Sodium Leak Channel (NALCN) Lead to Distal Arthrogryposis with Increased Muscle Tone. Neuropediatrics. 2016;47: 273–277. doi:10.1055/s-0036-1584084

27. Köroğlu Ç, Seven M, Tolun A. Recessive truncating NALCN mutation in infantile neuroaxonal dystrophy with facial dysmorphism. J Med Genet. 2013;50: 515–520. doi:10.1136/jmedgenet-2013-101634

- 521 28. Perez Y, Kadir R, Volodarsky M, Noyman I, Flusser H, Shorer Z, et al. UNC80 mutation causes a
522 syndrome of hypotonia, severe intellectual disability, dyskinesia and dysmorphism, similar to
523 that caused by mutations in its interacting cation channel NALCN. J Med Genet. 2016;53: 397–
524 402. doi:10.1136/jmedgenet-2015-103352
- 525 29. Valkanas E, Schaffer K, Dunham C, Maduro V, du Souich C, Rupps R, et al. Phenotypic evolution of
526 UNC80 loss of function. Am J Med Genet A. 2016;170: 3106–3114. doi:10.1002/ajmg.a.37929
- 527 30. Shamseldin HE, Faqeih E, Alasmari A, Zaki MS, Gleeson JG, Alkuraya FS. Mutations in UNC80,
528 Encoding Part of the UNC79-UNC80-NALCN Channel Complex, Cause Autosomal-Recessive
529 Severe Infantile Encephalopathy. Am J Hum Genet. 2016;98: 210–215.
530 doi:10.1016/j.ajhg.2015.11.013
- 531 31. Stray-Pedersen A, Cobben J-M, Prescott TE, Lee S, Cang C, Aranda K, et al. Biallelic Mutations in
532 UNC80 Cause Persistent Hypotonia, Encephalopathy, Growth Retardation, and Severe
533 Intellectual Disability. Am J Hum Genet. 2016;98: 202–209. doi:10.1016/j.ajhg.2015.11.004
- 534 32. Wang Y, Koh K, Ichinose Y, Yasumura M, Ohtsuka T, Takiyama Y. A de novo mutation in the
535 NALCN gene in an adult patient with cerebellar ataxia associated with intellectual disability and
536 arthrogryposis. Clin Genet. 2016;90: 556–557. doi:10.1111/cge.12851
- 537 33. Lozic B, Johansson S, Lovric Kojundzic S, Markic J, Knappskog PM, Hahn AF, et al. Novel NALCN
538 variant: altered respiratory and circadian rhythm, anesthetic sensitivity. Ann Clin Transl Neurol.
539 2016;3: 876–883. doi:10.1002/acn3.362
- 540 34. Funato H, Miyoshi C, Fujiyama T, Kanda T, Sato M, Wang Z, et al. Forward-genetics analysis of
541 sleep in randomly mutagenized mice. Nature. 2016;539: 378–383. doi:10.1038/nature20142

- 542 35. Humphrey JA, Hamming KS, Thacker CM, Scott RL, Sedensky MM, Snutch TP, et al. A putative
543 cation channel and its novel regulator: cross-species conservation of effects on general
544 anesthesia. *Curr Biol.* 2007;17: 624–629. doi:10.1016/j.cub.2007.02.037
- 545 36. Jospin M, Watanabe S, Joshi D, Young S, Hamming K, Thacker C, et al. UNC-80 and the NCA ion
546 channels contribute to endocytosis defects in synaptojanin mutants. *Curr Biol.* 2007;17: 1595–
547 1600. doi:10.1016/j.cub.2007.08.036
- 548 37. Nash HA, Scott RL, Lear BC, Allada R. An unusual cation channel mediates photic control of
549 locomotion in *Drosophila*. *Curr Biol.* 2002;12: 2152–2158.
- 550 38. Pierce-Shimomura JT, Chen BL, Mun JJ, Ho R, Sarkis R, McIntire SL. Genetic analysis of crawling
551 and swimming locomotory patterns in *C. elegans*. *Proc Natl Acad Sci U S A.* 2008;105: 20982–
552 20987. doi:10.1073/pnas.0810359105
- 553 39. Yeh E, Ng S, Zhang M, Bouhours M, Wang Y, Wang M, et al. A putative cation channel, NCA-1, and
554 a novel protein, UNC-80, transmit neuronal activity in *C. elegans*. *PLoS Biol.* 2008;6: e55.
555 doi:10.1371/journal.pbio.0060055
- 556 40. Lear BC, Darrah EJ, Aldrich BT, Gebre S, Scott RL, Nash HA, et al. UNC79 and UNC80, Putative
557 Auxiliary Subunits of the NARROW ABDOMEN Ion Channel, Are Indispensable for Robust
558 Circadian Locomotor Rhythms in *Drosophila*. *PloS One.* 2013;8: e78147.
559 doi:10.1371/journal.pone.0078147
- 560 41. Lear BC, Lin J-M, Keath JR, McGill JJ, Raman IM, Allada R. The ion channel narrow abdomen is
561 critical for neural output of the *Drosophila* circadian pacemaker. *Neuron.* 2005;48: 965–976.
562 doi:10.1016/j.neuron.2005.10.030

- 563 42. Lu B, Su Y, Das S, Wang H, Wang Y, Liu J, et al. Peptide neurotransmitters activate a cation
564 channel complex of NALCN and UNC-80. *Nature*. 2009;457: 741–744. doi:10.1038/nature07579
- 565 43. Swayne LA, Mezghrani A, Varrault A, Chemin J, Bertrand G, Dalle S, et al. The NALCN ion channel
566 is activated by M3 muscarinic receptors in a pancreatic beta-cell line. *EMBO Rep*. 2009;10: 873–
567 880. doi:10.1038/embor.2009.125
- 568 44. Lu B, Zhang Q, Wang H, Wang Y, Nakayama M, Ren D. Extracellular calcium controls background
569 current and neuronal excitability via an UNC79-UNC80-NALCN cation channel complex. *Neuron*.
570 2010;68: 488–499. doi:10.1016/j.neuron.2010.09.014
- 571 45. Fukuto HS, Ferkey DM, Apicella AJ, Lans H, Sharmeen T, Chen W, et al. G protein-coupled receptor
572 kinase function is essential for chemosensation in *C. elegans*. *Neuron*. 2004;42: 581–593.
- 573 46. Doi M, Iwasaki K. Regulation of retrograde signaling at neuromuscular junctions by the novel C2
574 domain protein AEX-1. *Neuron*. 2002;33: 249–259.
- 575 47. Ailion M, Hannemann M, Dalton S, Pappas A, Watanabe S, Hegermann J, et al. Two Rab2
576 interactors regulate dense-core vesicle maturation. *Neuron*. 2014;82: 167–180.
577 doi:10.1016/j.neuron.2014.02.017
- 578 48. Vidal-Gadea A, Topper S, Young L, Crisp A, Kressin L, Elbel E, et al. *Caenorhabditis elegans* selects
579 distinct crawling and swimming gaits via dopamine and serotonin. *Proc Natl Acad Sci U S A*.
580 2011;108: 17504–17509. doi:10.1073/pnas.1108673108
- 581 49. Pitcher JA, Freedman NJ, Lefkowitz RJ. G protein-coupled receptor kinases. *Annu Rev Biochem*.
582 1998;67: 653–692. doi:10.1146/annurev.biochem.67.1.653
- 583 50. Evron T, Daigle TL, Caron MG. GRK2: multiple roles beyond G protein-coupled receptor
584 desensitization. *Trends Pharmacol Sci*. 2012;33: 154–164. doi:10.1016/j.tips.2011.12.003

- 585 51. Ribas C, Penela P, Murga C, Salcedo A, García-Hoz C, Jurado-Pueyo M, et al. The G protein-coupled
586 receptor kinase (GRK) interactome: role of GRKs in GPCR regulation and signaling. *Biochim*
587 *Biophys Acta*. 2007;1768: 913–922. doi:10.1016/j.bbamem.2006.09.019
- 588 52. Kong G, Penn R, Benovic JL. A beta-adrenergic receptor kinase dominant negative mutant
589 attenuates desensitization of the beta 2-adrenergic receptor. *J Biol Chem*. 1994;269: 13084–
590 13087.
- 591 53. Wood JF, Wang J, Benovic JL, Ferkey DM. Structural domains required for *Caenorhabditis elegans*
592 G protein-coupled receptor kinase 2 (GRK-2) function in vivo. *J Biol Chem*. 2012;287: 12634–
593 12644. doi:10.1074/jbc.M111.336818
- 594 54. Pao CS, Barker BL, Benovic JL. Role of the amino terminus of G protein-coupled receptor kinase 2
595 in receptor phosphorylation. *Biochemistry*. 2009;48: 7325–7333. doi:10.1021/bi900408g
- 596 55. Boguth CA, Singh P, Huang C, Tesmer JJG. Molecular basis for activation of G protein-coupled
597 receptor kinases. *EMBO J*. 2010;29: 3249–3259. doi:10.1038/emboj.2010.206
- 598 56. Huang C, Yoshino-Koh K, Tesmer JJG. A surface of the kinase domain critical for the allosteric
599 activation of G protein-coupled receptor kinases. *J Biol Chem*. 2009;284: 17206–17215.
600 doi:10.1074/jbc.M809544200
- 601 57. Huang C-C, Orban T, Jastrzebska B, Palczewski K, Tesmer JJG. Activation of G protein-coupled
602 receptor kinase 1 involves interactions between its N-terminal region and its kinase domain.
603 *Biochemistry*. 2011;50: 1940–1949. doi:10.1021/bi101606e
- 604 58. Noble B, Kallal LA, Pausch MH, Benovic JL. Development of a yeast bioassay to characterize G
605 protein-coupled receptor kinases. Identification of an NH2-terminal region essential for receptor
606 phosphorylation. *J Biol Chem*. 2003;278: 47466–47476. doi:10.1074/jbc.M308257200

- 607 59. Pao CS, Benovic JL. Phosphorylation-independent desensitization of G protein-coupled
608 receptors? Sci STKE. 2002;2002: pe42. doi:10.1126/stke.2002.153.pe42
- 609 60. Sterne-Marr R, Tesmer JJG, Day PW, Stracquatano RP, Cilente J-AE, O'Connor KE, et al. G protein-
610 coupled receptor Kinase 2/G alpha q/11 interaction. A novel surface on a regulator of G protein
611 signaling homology domain for binding G alpha subunits. J Biol Chem. 2003;278: 6050–6058.
612 doi:10.1074/jbc.M208787200
- 613 61. Boekhoff I, Inglese J, Schleicher S, Koch WJ, Lefkowitz RJ, Breer H. Olfactory desensitization
614 requires membrane targeting of receptor kinase mediated by beta gamma-subunits of
615 heterotrimeric G proteins. J Biol Chem. 1994;269: 37–40.
- 616 62. Koch WJ, Inglese J, Stone WC, Lefkowitz RJ. The binding site for the beta gamma subunits of
617 heterotrimeric G proteins on the beta-adrenergic receptor kinase. J Biol Chem. 1993;268: 8256–
618 8260.
- 619 63. Touhara K, Koch WJ, Hawes BE, Lefkowitz RJ. Mutational analysis of the pleckstrin homology
620 domain of the beta-adrenergic receptor kinase. Differential effects on G beta gamma and
621 phosphatidylinositol 4,5-bisphosphate binding. J Biol Chem. 1995;270: 17000–17005.
- 622 64. Carman CV, Barak LS, Chen C, Liu-Chen LY, Onorato JJ, Kennedy SP, et al. Mutational analysis of
623 Gbetagamma and phospholipid interaction with G protein-coupled receptor kinase 2. J Biol
624 Chem. 2000;275: 10443–10452.
- 625 65. Topalidou I, Cattin-Ortolá J, Pappas AL, Cooper K, Merrihew GE, MacCoss MJ, et al. The EARP
626 Complex and Its Interactor EIPR-1 Are Required for Cargo Sorting to Dense-Core Vesicles. PLoS
627 Genet. 2016;12: e1006074. doi:10.1371/journal.pgen.1006074

- 628 66. Koelle MR. Neurotransmitter signaling through heterotrimeric G proteins: insights from studies
629 in *C. elegans*. WormBook Online Rev C *Elegans Biol*. 2016; 1–78. doi:10.1895/wormbook.1.75.2
- 630 67. Bastiani CA, Gharib S, Simon MI, Sternberg PW. *Caenorhabditis elegans* Galphaq regulates egg-
631 laying behavior via a PLCbeta-independent and serotonin-dependent signaling pathway and
632 likely functions both in the nervous system and in muscle. *Genetics*. 2003;165: 1805–1822.
- 633 68. Brundage L, Avery L, Katz A, Kim UJ, Mendel JE, Sternberg PW, et al. Mutations in a *C. elegans*
634 Gqalpha gene disrupt movement, egg laying, and viability. *Neuron*. 1996;16: 999–1009.
- 635 69. Mendel JE, Korswagen HC, Liu KS, Hajdu-Cronin YM, Simon MI, Plasterk RH, et al. Participation of
636 the protein Go in multiple aspects of behavior in *C. elegans*. *Science*. 1995;267: 1652–1655.
- 637 70. Ségalat L, Elkes DA, Kaplan JM. Modulation of serotonin-controlled behaviors by Go in
638 *Caenorhabditis elegans*. *Science*. 1995;267: 1648–1651.
- 639 71. Hajdu-Cronin YM, Chen WJ, Patikoglou G, Koelle MR, Sternberg PW. Antagonism between
640 G(o)alpha and G(q)alpha in *Caenorhabditis elegans*: the RGS protein EAT-16 is necessary for
641 G(o)alpha signaling and regulates G(q)alpha activity. *Genes Dev*. 1999;13: 1780–1793.
- 642 72. Nurrish S, Ségalat L, Kaplan JM. Serotonin inhibition of synaptic transmission: Galpha(0)
643 decreases the abundance of UNC-13 at release sites. *Neuron*. 1999;24: 231–242.
- 644 73. Sawin ER, Ranganathan R, Horvitz HR. *C. elegans* locomotory rate is modulated by the
645 environment through a dopaminergic pathway and by experience through a serotonergic
646 pathway. *Neuron*. 2000;26: 619–631.
- 647 74. Lints R, Emmons SW. Patterning of dopaminergic neurotransmitter identity among
648 *Caenorhabditis elegans* ray sensory neurons by a TGFbeta family signaling pathway and a Hox
649 gene. *Development*. 1999;126: 5819–5831.

- 650 75. Chase DL, Pepper JS, Koelle MR. Mechanism of extrasynaptic dopamine signaling in
651 Caenorhabditis elegans. Nat Neurosci. 2004;7: 1096–1103. doi:10.1038/nn1316
- 652 76. Xie L, Gao S, Alcaire SM, Aoyagi K, Wang Y, Griffin JK, et al. NLF-1 delivers a sodium leak channel
653 to regulate neuronal excitability and modulate rhythmic locomotion. Neuron. 2013;77: 1069–
654 1082. doi:10.1016/j.neuron.2013.01.018
- 655 77. Koelle MR, Horvitz HR. EGL-10 regulates G protein signaling in the C. elegans nervous system and
656 shares a conserved domain with many mammalian proteins. Cell. 1996;84: 115–125.
- 657 78. Ezak MJ, Ferkey DM. The C. elegans D2-like dopamine receptor DOP-3 decreases behavioral
658 sensitivity to the olfactory stimulus 1-octanol. PloS One. 2010;5: e9487.
659 doi:10.1371/journal.pone.0009487
- 660 79. Ferkey DM, Hyde R, Haspel G, Dionne HM, Hess HA, Suzuki H, et al. C. elegans G protein regulator
661 RGS-3 controls sensitivity to sensory stimuli. Neuron. 2007;53: 39–52.
662 doi:10.1016/j.neuron.2006.11.015
- 663 80. Wragg RT, Hapiak V, Miller SB, Harris GP, Gray J, Komuniecki PR, et al. Tyramine and octopamine
664 independently inhibit serotonin-stimulated aversive behaviors in Caenorhabditis elegans
665 through two novel amine receptors. J Neurosci. 2007;27: 13402–13412.
666 doi:10.1523/JNEUROSCI.3495-07.2007
- 667 81. Cho D, Zheng M, Min C, Ma L, Kurose H, Park JH, et al. Agonist-induced endocytosis and receptor
668 phosphorylation mediate resensitization of dopamine D(2) receptors. Mol Endocrinol. 2010;24:
669 574–586. doi:10.1210/me.2009-0369
- 670 82. Gurevich EV, Gainetdinov RR, Gurevich VV. G protein-coupled receptor kinases as regulators of
671 dopamine receptor functions. Pharmacol Res. 2016;111: 1–16. doi:10.1016/j.phrs.2016.05.010

- 672 83. Ito K, Haga T, Lamah J, Sadée W. Sequestration of dopamine D2 receptors depends on
673 coexpression of G-protein-coupled receptor kinases 2 or 5. Eur J Biochem. 1999;260: 112–119.
674 doi:10.1046/j.1432-1327.1999.00125.x
- 675 84. Kim KM, Valenzano KJ, Robinson SR, Yao WD, Barak LS, Caron MG. Differential regulation of the
676 dopamine D2 and D3 receptors by G protein-coupled receptor kinases and beta-arrestins. J Biol
677 Chem. 2001;276: 37409–37414. doi:10.1074/jbc.M106728200
- 678 85. Namkung Y, Dipace C, Urizar E, Javitch JA, Sibley DR. G protein-coupled receptor kinase-2
679 constitutively regulates D2 dopamine receptor expression and signaling independently of
680 receptor phosphorylation. J Biol Chem. 2009;284: 34103–34115. doi:10.1074/jbc.M109.055707
- 681 86. Namkung Y, Dipace C, Javitch JA, Sibley DR. G protein-coupled receptor kinase-mediated
682 phosphorylation regulates post-endocytic trafficking of the D2 dopamine receptor. J Biol Chem.
683 2009;284: 15038–15051. doi:10.1074/jbc.M900388200
- 684 87. Daigle TL, Ferris MJ, Gainetdinov RR, Sotnikova TD, Urs NM, Jones SR, et al. Selective deletion of
685 GRK2 alters psychostimulant-induced behaviors and dopamine neurotransmission.
686 Neuropsychopharmacol. 2014;39: 2450–2462. doi:10.1038/npp.2014.97
- 687 88. Miller KG, Emerson MD, Rand JB. Gqalpha and diacylglycerol kinase negatively regulate the
688 Gqalpha pathway in *C. elegans*. Neuron. 1999;24: 323–333.
- 689 89. Gao S, Xie L, Kawano T, Po MD, Pirri JK, Guan S, et al. The NCA sodium leak channel is required for
690 persistent motor circuit activity that sustains locomotion. Nat Commun. 2015;6: 6323.
691 doi:10.1038/ncomms7323
- 692 90. Brenner S. The genetics of *Caenorhabditis elegans*. Genetics. 1974;77: 71–94.

- 693 91. Minevich G, Park DS, Blankenberg D, Poole RJ, Hobert O. CloudMap: a cloud-based pipeline for
694 analysis of mutant genome sequences. *Genetics*. 2012;192: 1249–1269.
695 doi:10.1534/genetics.112.144204
- 696 92. Frøkjaer-Jensen C, Davis MW, Hopkins CE, Newman BJ, Thummel JM, Olesen S-P, et al. Single-
697 copy insertion of transgenes in *Caenorhabditis elegans*. *Nat Genet*. 2008;40: 1375–1383.
698 doi:10.1038/ng.248
- 699 93. Frøkjær-Jensen C, Davis MW, Ailion M, Jorgensen EM. Improved Mos1-mediated transgenesis in
700 *C. elegans*. *Nat Methods*. 2012;9: 117–118. doi:10.1038/nmeth.1865
- 701 94. Mello CC, Kramer JM, Stinchcomb D, Ambros V. Efficient gene transfer in *C.elegans*:
702 extrachromosomal maintenance and integration of transforming sequences. *EMBO J*. 1991;10:
703 3959–3970.

Figure Captions

Fig 1. The GRK-2 kinase regulates locomotion and G_q signaling.

(A,B) A *grk-2* mutation suppresses activated G_q. The activated G_q mutant *egl-30(tg26)* (G_q^{*}) has hyperactive locomotion and deep body bends. The *grk-2(gk268)* mutation suppresses both the deep body bends (A) and hyperactive locomotion (B) of activated G_q. (***, P<0.001. Error bars = SEM; n = 10).

(C) The kinase activity of GRK-2 is required for proper locomotion. The *grk-2(gk268)* mutant has slow locomotion that is rescued by expression of the wild-type *grk-2* cDNA under the control of its own promoter GRK-2(+), but is not rescued by expression of the kinase dead GRK-2[K220R]. (***, P<0.001. Error bars = SEM; n = 10).

(D) The kinase activity of GRK-2 is required for suppression of activated G_q. A *grk-2(gk268)* mutation suppresses the hyperactive locomotion of *egl-30(tg26)* (G_q^{*}). Expression of the kinase dead GRK-2[K220R] does not rescue the *grk-2* mutant for this phenotype. (**, P<0.01. Error bars = SEM; n = 10).

Fig 2. GRK-2 regulation of locomotion requires GPCR-phosphorylation and membrane association.

(A) Domain structure of GRK-2. GRK-2 is a 707 amino acid protein with three well-characterized domains: the RGS homology (RH) domain, the kinase domain and the pleckstrin homology (PH) domain. The protein structure was drawn using DOG 1.0.

(B-D) Residues required for GPCR phosphorylation are required for GRK-2 function in locomotion. The D3K (transgene *yakEx77*), L4K (transgene *yakEx78*), V7A/L8A (transgene *yakEx79*), and D10A (transgene *yakEx80*) mutations are predicted to block GPCR phosphorylation. The R195A mutation (transgene *yakEx95*) disrupts predicted intramolecular stabilizing interactions which are required for effective phosphorylation. In each case, expression of the mutated *grk-2* cDNA under the control of its own promoter did not restore the slow locomotion of *grk-2(gk268)* mutants (ns, P>0.05, each strain compared to *grk-2*. Error bars = SEM; n = 10-20).

(E) Residues in the RH domain predicted to disrupt G_q binding are not required for GRK-2 function in locomotion. The R106A (transgene *yakEx57*), Y109I (transgene *yakEx55*), and D110A (transgene *yakEx56*) mutations are predicted to disrupt G_q binding. In each case expression of the mutated *grk-2* cDNA under the control of the *grk-2* promoter significantly rescued the slow locomotion of *grk-2(gk268)* mutants (**, $P < 0.01$; ***, $P < 0.001$. Error bars = SEM; $n = 10$).

(F) Residues in the PH domain predicted to disrupt GRK-2 phospholipid binding or binding to $G\beta\gamma$ are required for GRK-2 function in locomotion. Mutation K567E (transgene *yakEx87*) is predicted to disrupt GRK-2 phospholipid binding, and mutation R587Q (transgene *yakEx88*) is predicted to disrupt binding to $G\beta\gamma$. In both cases, expression of the mutated *grk-2* cDNA under the control of the *grk-2* promoter did not restore the slow locomotion of *grk-2(gk268)* mutants. (**, $P < 0.01$. ns, $P > 0.05$. Error bars = SEM; $n = 10$).

Fig 3. GRK-2 acts in head acetylcholine neurons.

(A) *grk-2* acts in head acetylcholine neurons to control locomotion. The *grk-2* cDNA was expressed in *grk-2(gk268)* mutants under a pan-neuronal promoter (*Prab-3*, transgene *yakEx44*), acetylcholine neuron promoter (*Punc-17*, transgene *yakEx45*), ventral cord acetylcholine motor neuron promoter (*Pacr-2*, transgene *yakEx47*), head acetylcholine neuron promoter (*Punc-17H*, transgene *yakEx51*), glutamate receptor promoter (*Pglr-1*, transgene *yakEx52*), and ciliated sensory neuron promoter (*Pxbx-1*, transgene *yakEx71*). Expression driven by the pan-neuronal, acetylcholine neuron, and head acetylcholine neuron promoters rescued the slow locomotion of *grk-2* mutants. (***, $P < 0.001$. Error bars = SEM; $n = 10-25$).

(B,C) GRK-2 acts in head acetylcholine neurons to positively regulate G_q . A *grk-2(gk268)* mutant suppresses the deep body bends and hyperactive locomotion of the activated G_q mutant *egl-30(tg26)* (G_q^*). Expression of the *grk-2* cDNA under a head acetylcholine neuron promoter (*Punc-17H*, transgene *yakEx51*) rescues the *grk-2* suppression of the deep body bends (B) and hyperactive locomotion (C) of activated G_q . (***, $P < 0.001$. Error bars = SEM; $n = 10$).

(D) *grk-2* is expressed in head acetylcholine neurons. Representative images of a z-stack projection of animals coexpressing tagRFP fused to the GRK-2 ORF under the *grk-2* promoter (*grk-2::tagRFP*, integration *yakIs19*) and GFP under a head acetylcholine neuron promoter (*Punc-17H::eGFP*, transgene *yakEx94*). Scale bar: 10 μ m.

Fig 4. Mutations in *dop-3* and *cat-2* suppress *grk-2*.

(A) Mutations in *dop-3* and *cat-2* suppress the slow locomotion of *grk-2* mutants. *grk-2(gk268)* mutants have a slow locomotion phenotype. The *dop-3(vs106)* mutation fully suppresses and the *cat-2(e1112)* mutation partially suppresses the slow locomotion of *grk-2(gk268)* mutants (***, $P < 0.001$. Error bars = SEM; $n = 32-72$).

(B,C) A *dop-3* mutation suppresses the *grk-2* mutant suppression of activated G_q . The *grk-2(gk268)* mutation suppresses the deep body bends and hyperactive locomotion of the activated G_q mutant *egl-30(tg26)* (G_q^*). The *dop-3(vs106)* mutation suppresses the *grk-2* suppression of the deep body bends (B) and hyperactive locomotion (C) of G_q^* . (***, $P < 0.001$. Error bars = SEM; $n = 15-20$).

(D,E) A *cat-2* mutation suppresses the *grk-2* mutant suppression of activated G_q . The *grk-2(gk268)* mutation suppresses the deep body bends and hyperactive locomotion of the activated G_q mutant *egl-30(tg26)* (G_q^*). The *cat-2(e1112)* mutation suppresses the *grk-2* suppression of the deep body bends (D) and hyperactive locomotion (E) of G_q^* . (***, $P < 0.001$. Error bars = SEM; $n = 15-20$).

(F) *grk-2* mutants are hypersensitive to dopamine in a *dop-3*-dependent manner. Shown is the percentage of wild type, *dop-3(vs106)*, *grk-2(gk268)*, or *grk-2(gk268); dop-3(vs106)* animals that moved ten body bends after a 20 min exposure to the indicated concentrations of dopamine. Every data point represents the mean \pm SEM for two trials (15-20 animals per experiment and strain).

Fig 5. GRK-2 is a positive regulator of NCA-1 and NCA-2 channel activity.

(A) A *grk-2* mutation enhances the weak forward fainting phenotype of an *nlf-1* mutant. Representative images of wild-type, *nlf-1(tm3631)*, and *grk-2(gk268); nlf-1(tm3631)* mutant animals. The asterisk shows the characteristic straight posture of the head when an animal faints.

(B) A *grk-2* mutation enhances the weak forward fainting phenotype of an *nlf-1* mutant. The *nlf-1(tm3631)* mutant is a weak fainter. The *grk-2(gk268)* mutation enhances the *nlf-1* mutant so that the double is a strong fainter. (***, $P < 0.001$. Error bars = SEM; $n = 10-20$). The number shown is the number of body bends before the animal faints. If the animal made ten body bends without fainting, the assay was stopped and we recorded ten as the number (see Methods for details).

(C) The *grk-2(gk268)* mutation enhances the *unc-73(ox317)* mutant so that the double mutant is a strong fainter. The *grk-2(gk268)* mutation has no effect on an *egl-8(sa47)* mutant. (***, $P < 0.001$. Error bars = SEM; $n = 15$).

(D) The *egl-10(md176)* mutation enhances the *nlf-1(tm3631)* mutant so that the double mutant is a strong fainter. (***, $P < 0.001$. Error bars = SEM; $n = 25$).

(E) Expression of activated G_o in head acetylcholine neurons inhibits locomotion. Animals expressing an activated G_o mutant (GOA-1[Q205L]) under a head acetylcholine neuron promoter (*Punc-17H::GOA-1**, transgene *yakEx103*) move more slowly than wild type animals. (***, $P < 0.001$. Error bars = SEM; $n = 17$).

(F) Expression of activated G_o in head acetylcholine neurons enhances the weak forward fainting phenotype of an *nlf-1* mutant. The *nlf-1(tm3631)* mutant is a weak fainter in forward movement. The *nlf-1(tm3631)* mutant expressing an activated G_o mutant (GOA-1[Q205L]) under a head acetylcholine neuron promoter (*Punc-17H::GOA-1**; transgene *yakEx103*) is a stronger fainter than the *nlf-1(tm3631)* mutant. (***, $P < 0.001$. Error bars = SEM; $n = 54$).

Fig 6. Dopamine negatively regulates NCA-1 and NCA-2 channel activity.

(A) The *cat-2(e1112)* mutation suppresses the weak forward fainting phenotype of the *nlf-1(tm3631)* mutant. (***, $P < 0.001$. Error bars = SEM; $n = 40$).

(B) The *dop-3(vs106)* mutation suppresses the weak forward fainting phenotype of the *nlf-1(tm3631)* mutant. (***, $P < 0.001$. Error bars = SEM; $n = 40$).

(C) The *dop-3(vs106)* mutation partially suppresses the strong forward fainting phenotype of the *grk-2(gk268); nlf-1(tm3631)* double mutant. (***, $P < 0.001$. Error bars = SEM; $n = 40$).

(D) Exogenous dopamine causes the *grk-2(gk268)* mutant to faint in a *dop-3(vs106)* dependent manner. Shown is the percentage of animals that faint within a period of ten body bends when moving backwards after exposure to 2 mM dopamine for 20 min. (***, $P < 0.001$. Error bars = SEM; $n = 2-5$ trials of 14-25 animals each).

Fig 7. Model for GRK-2 and dopamine action in regulating activity of the NCA channels.

Schematic representation of the dopamine, G_q and G_o signaling pathways [66,75]. Intact arrows indicate direct actions or direct physical interactions. Dashed arrows indicate interactions that may be indirect. Our results suggest that dopamine decreases activity of the NCA-1 and NCA-2 channels (shown here collectively as “NCA”) by binding to DOP-3 and activating G_o signaling. GRK-2 acts as a kinase for the D2-like dopamine receptor DOP-3 to inhibit DOP-3, and thereby inhibit G_o , activate G_q , and positively regulate NCA-1 and NCA-2 channel activity.

817 **Supporting information**

818 **S1 Fig. *grk-2* mutant phenotypes.**

819 (A) The *grk-2(yak18)* mutation suppresses the deep body bends of the activated G_q mutant *egl-30(tg26)*
820 (*Gq**).

821 (B) The *grk-2(yak18)* mutant has slow locomotion (***, *P*<0.001. Error bars = SEM; *n* = 15).

822 (C) The *grk-2(gk268)* mutant has an egg-laying defect. The graph shows the number of eggs laid by 5
823 animals in a 2 h period. (**, *P*<0.01. Error bars = SEM; *n* = 2 plates of 5 animals each).

824 (D) The *grk-2(gk268)* mutant animals have short bodies. (***, *P*<0.001. Error bars = SEM; *n* = 10).

825 (E) A *dop-3* mutation does not suppress the restricted exploration behavior of *grk-2* mutants. Shown are
826 images of tracks of five wild-type, *grk-2(gk268)*, and *grk-2(gk268); dop-3(vs106)* mutant animals that were
827 allowed to explore a bacterial lawn for 2 hours at room temperature.

828

829 **S2 Fig. *grk-2* mutants have swimming defects.**

830 Shown are plots of bending angle (midpoint) versus time for representative individual animals. The two
831 plots of *grk-2(gk268)* mutant animals show individuals with strong and weak swimming defects. The *dop-*
832 *3(vs106)* mutation suppresses the swimming defects of the *grk-2(gk268)* mutant.

833

834 **S3 Fig. Arrestin mutants do not have locomotion defects.**

835 The *arr-1(ok401)* mutant has no locomotion defect. (ns, *P*>0.05. Error bars = SEM; *n* = 10).

836

837 **S4 Fig. A *grk-2* mutation suppresses the hyperactive locomotion of *dgk-1*, but not *goa-1* or *eat-16*** 838 **mutants.**

(A) A *grk-2* mutation does not suppress *goa-1* or *eat-16* mutants. The *eat-16(sa609)* and *goa-1(sa734)* mutants have a hyperactive locomotion phenotype. The *grk-2(gk268)* mutation does not suppress the hyperactive locomotion of *eat-16(sa609)* or *goa-1(sa734)*. (ns, $P > 0.05$. Error bars = SEM; $n = 10-20$).

(B) A *grk-2* mutation suppresses a *dgk-1* mutant. The *dgk-1(sy428)* mutant has a hyperactive locomotion phenotype. The *grk-2(gk268)* mutation suppresses the hyperactive locomotion of the *dgk-1(sy428)* mutant. (***, $P < 0.001$. ns, $P > 0.05$. Error bars = SEM; $n = 10-20$).

(C) *grk-2* requires its kinase activity to suppress the *dgk-1* hyperactive locomotion phenotype. The *grk-2(gk268)* mutation suppresses the hyperactive locomotion of the *dgk-1(sy428)* mutant. Expression of the kinase dead GRK-2[K220R] mutant under its own promoter (transgene *yakEx48*) does not rescue the *grk-2* suppression of *dgk-1* hyperactivity. (ns, $P > 0.05$. Error bars = SEM; $n = 10-20$).

(D) *grk-2* acts in head acetylcholine neurons to suppress the *dgk-1* hyperactive locomotion phenotype. Expression of the *grk-2* cDNA under a head acetylcholine neuron promoter (transgene *yakEx51*) rescues the *grk-2* suppression of the hyperactive locomotion of the *dgk-1(sy428)* mutant. (***, $P < 0.001$. Error bars = SEM; $n = 10-20$).

S5 Fig. *dop-3* acts in head acetylcholine neurons to regulate *grk-2* dependent locomotion.

(A) The *dop-3* suppression of *grk-2* is rescued by *dop-3* expression in head acetylcholine neurons. The *dop-3* cDNA was expressed in the *grk-2(gk268); dop-3(vs106)* double mutant under a pan-neuronal promoter (*Prab-3*, transgene *yakEx112*), acetylcholine neuron promoter (*Punc-17*, transgene *yakEx111*), head acetylcholine neuron promoter (*Punc-17H*, transgene *yakEx110*) and ventral cord acetylcholine motor neuron promoter (*Pacr-2*, transgene *yakEx109*). Expression of *dop-3* driven by the pan-neuronal, acetylcholine neuron, and head acetylcholine neuron promoters rescues the *dop-3(vs106)* mutant suppression of the slow locomotion of *grk-2(gk268)* mutant animals. (*, $P < 0.05$; **, $P < 0.01$; ***, $P < 0.001$; ns, $P > 0.05$. Error bars = SEM; $n = 10-33$).

(B) A *dop-1* mutation does not affect the *dop-3* suppression of the *grk-2* slow locomotion phenotype. *grk-2*; *dop-3* mutants move more rapidly than the *grk-2* mutant. The *dop-1(vs100)* mutation does not affect *grk-2(gk268)*; *dop-3(vs106)* locomotion. (ns, $P > 0.05$. Error bars = SEM; $n = 23-34$).

S6 Fig. A *grk-2* mutation partially suppresses activated Rho but does not suppress activated NCA-1.

(A,B) A *grk-2* mutation partially suppresses activated Rho. Animals expressing activated RHO-1 [RHO-1[G14V]] under an acetylcholine promoter (Rho*, transgene *nzIs29*) have slow locomotion and deep body bends. The *grk-2(gk268)* mutation partially suppresses both the deep body bends (A) and slow locomotion (B) of the Rho* animals. (***, $P < 0.001$. Error bars = SEM; $n = 10$).

(C,D) A *grk-2* mutation does not suppress activated NCA-1. The activated NCA-1 mutant (Nca*, *nca-1(ox352)*) has slow locomotion and deep body bends. The *grk-2(gk268)* mutation does not suppress the deep body bends (C) or the slow locomotion (D) of Nca*. To measure the locomotion of the slow moving Nca* animals, we used a radial locomotion assay in which we placed animals in the center of a 10 cm plate and measured how far the animals had moved in one hour. (ns, $P > 0.05$. Error bars = SEM; $n = 10$).

S7 Fig. Mutations in *dop-3* and *cat-2* do not suppress the strong fainter phenotype of *unc-80* mutants.

(A) The *dop-3(vs106)* mutation does not suppress the strong forward fainting phenotype of the *unc-80(ox330)* mutant. (ns, $P > 0.05$. Error bars = SEM; $n = 20$).

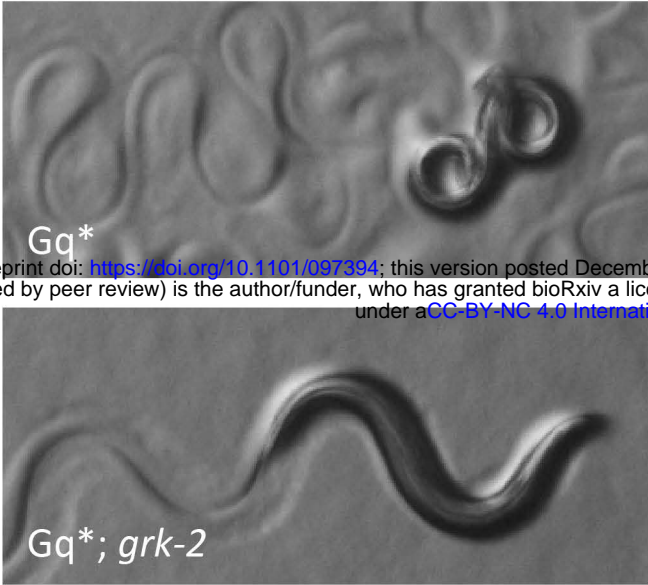
(B) The *cat-2(e1112)* mutation does not suppress the strong forward fainting phenotype of the *unc-80(ox330)* mutant. (ns, $P > 0.05$. Error bars = SEM; $n = 36-38$).

S1 Table. List of strains.

S2 Table. List of plasmids.

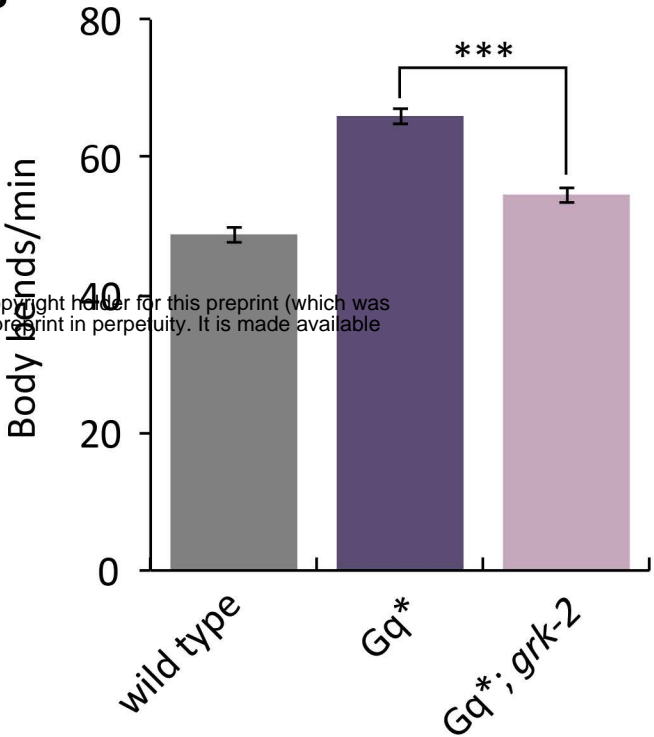
Fig 1

A

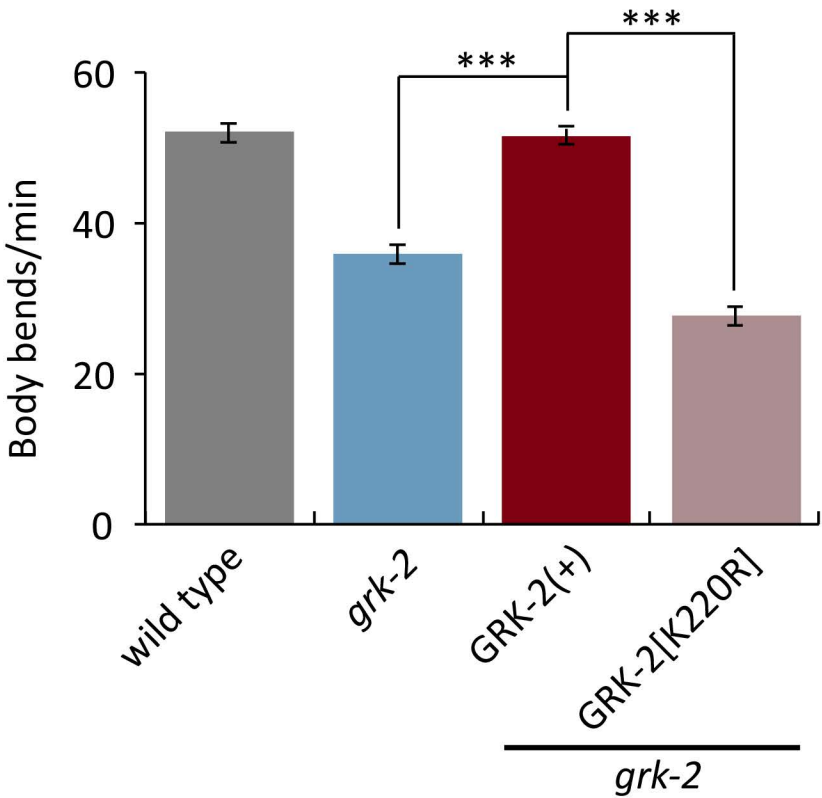


bioRxiv preprint doi: <https://doi.org/10.1101/097394>; this version posted December 30, 2016. The copyright holder for this preprint (which was not certified by peer review) is the author/funder, who has granted bioRxiv a license to display the preprint in perpetuity. It is made available under aCC-BY-NC 4.0 International license.

B



C



D

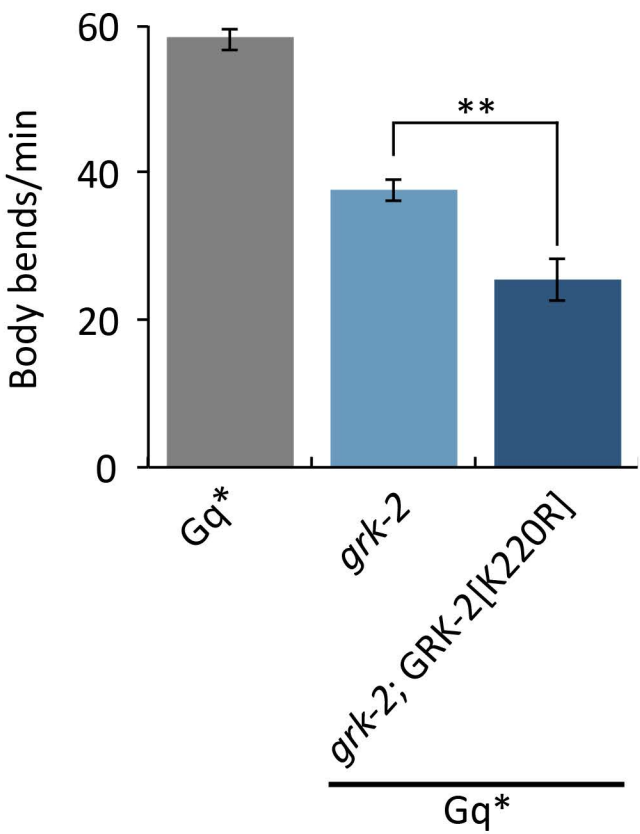


Fig 2

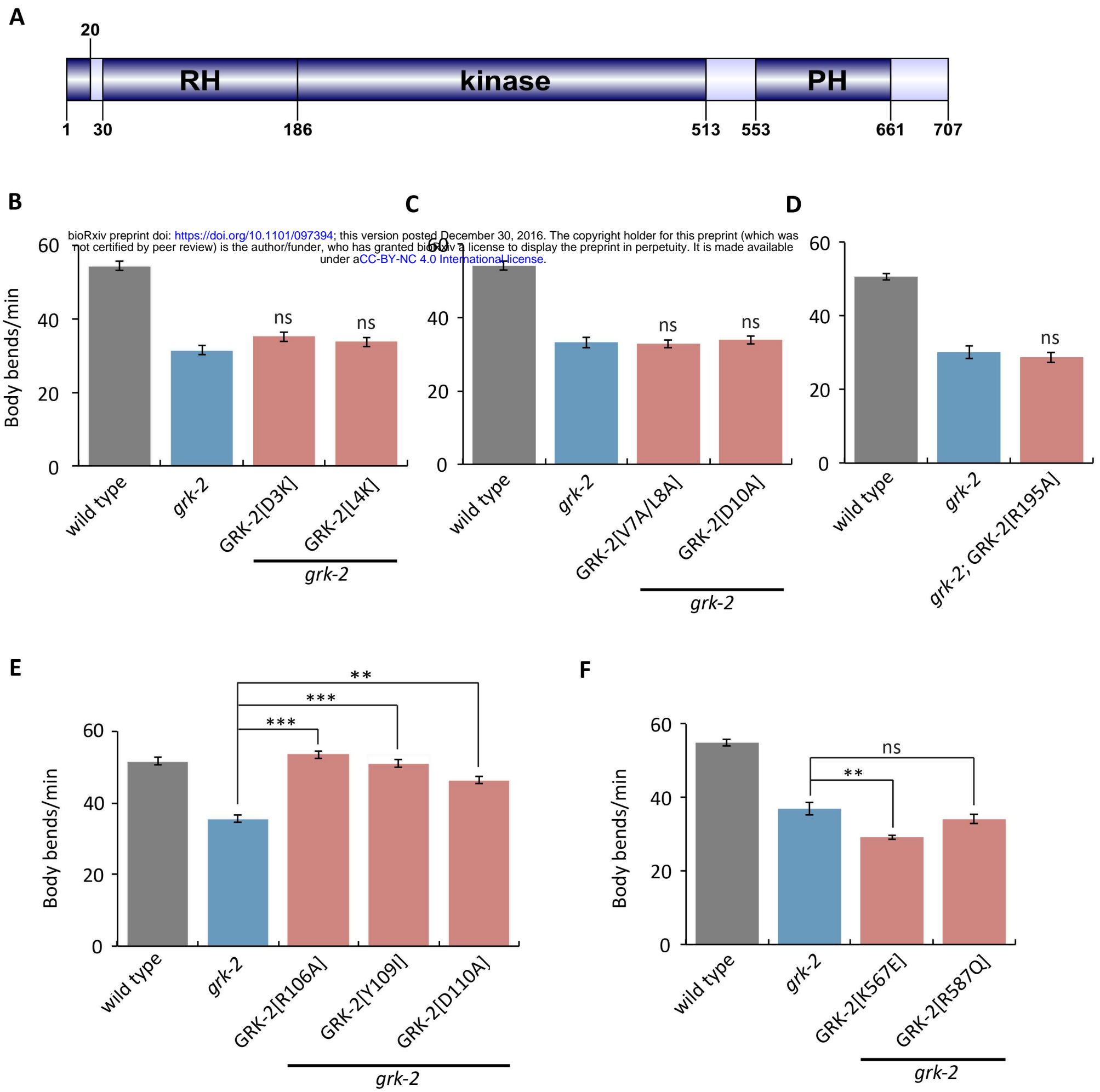


Fig 3

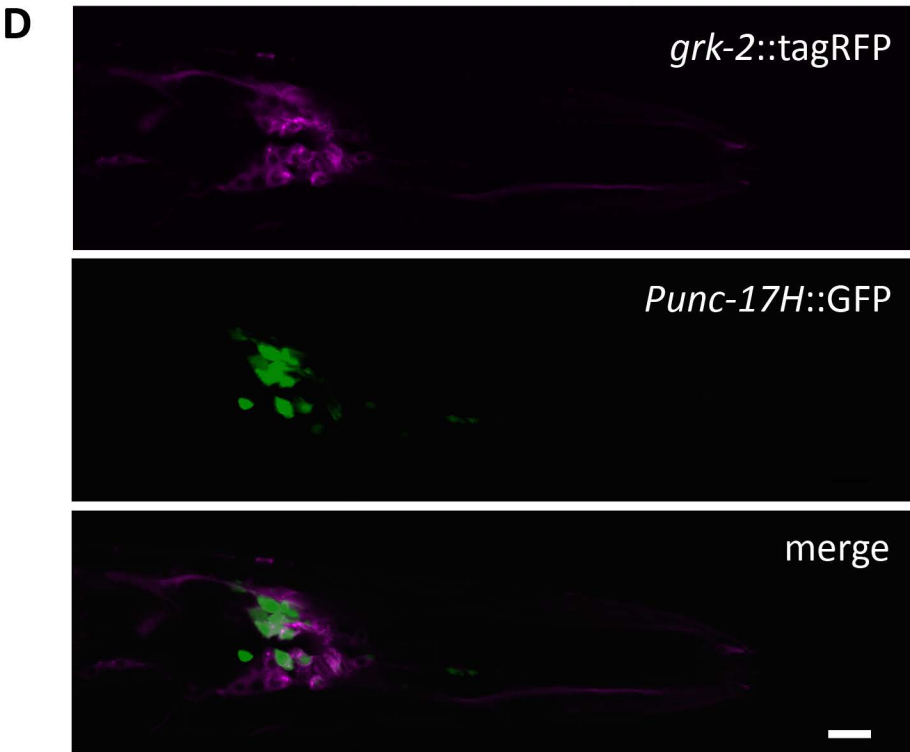
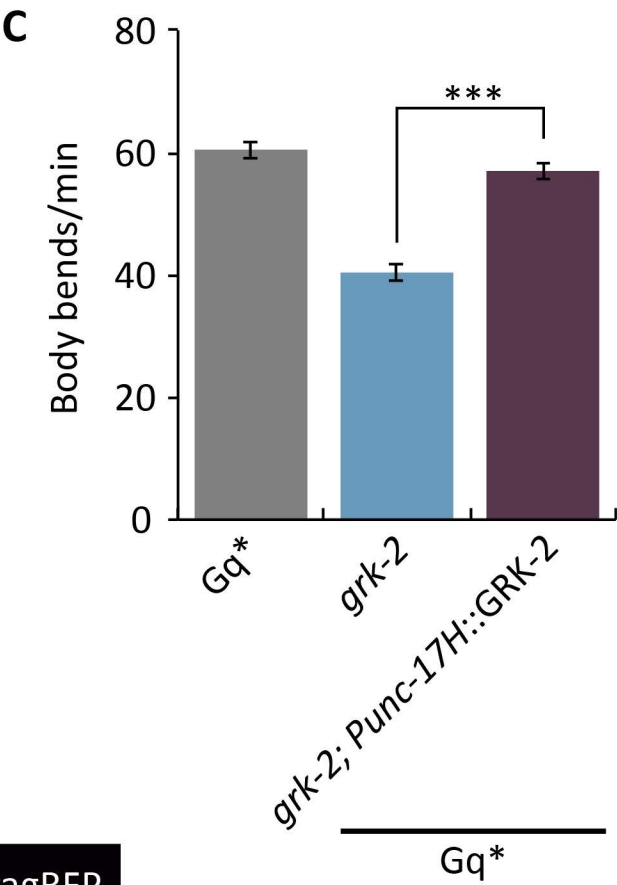
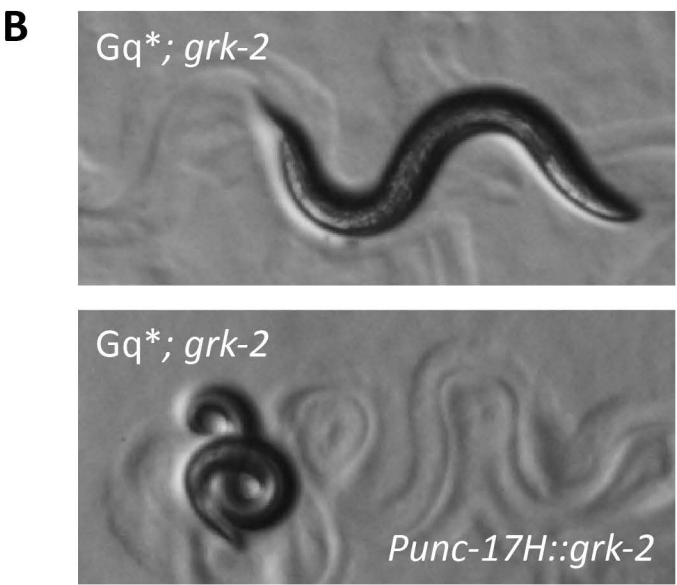
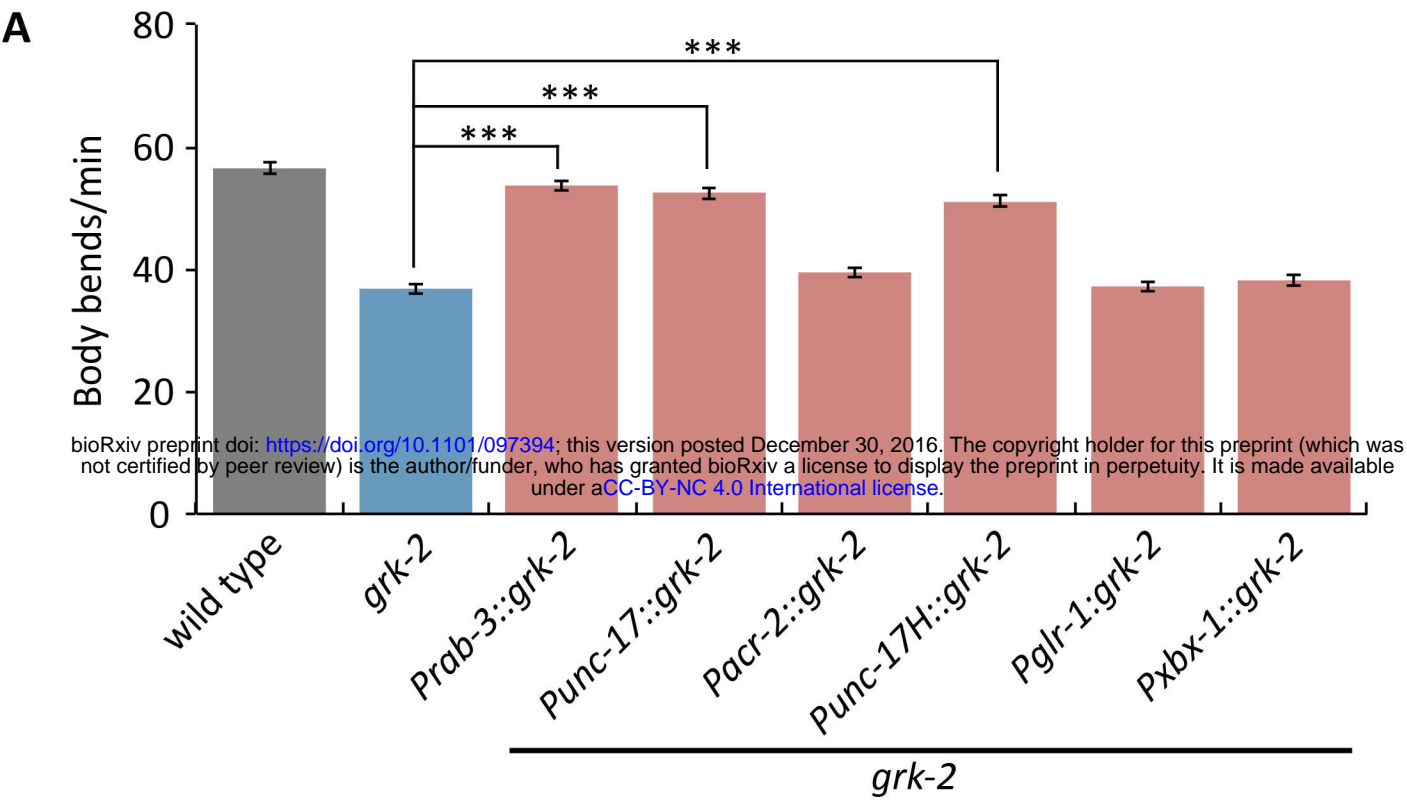
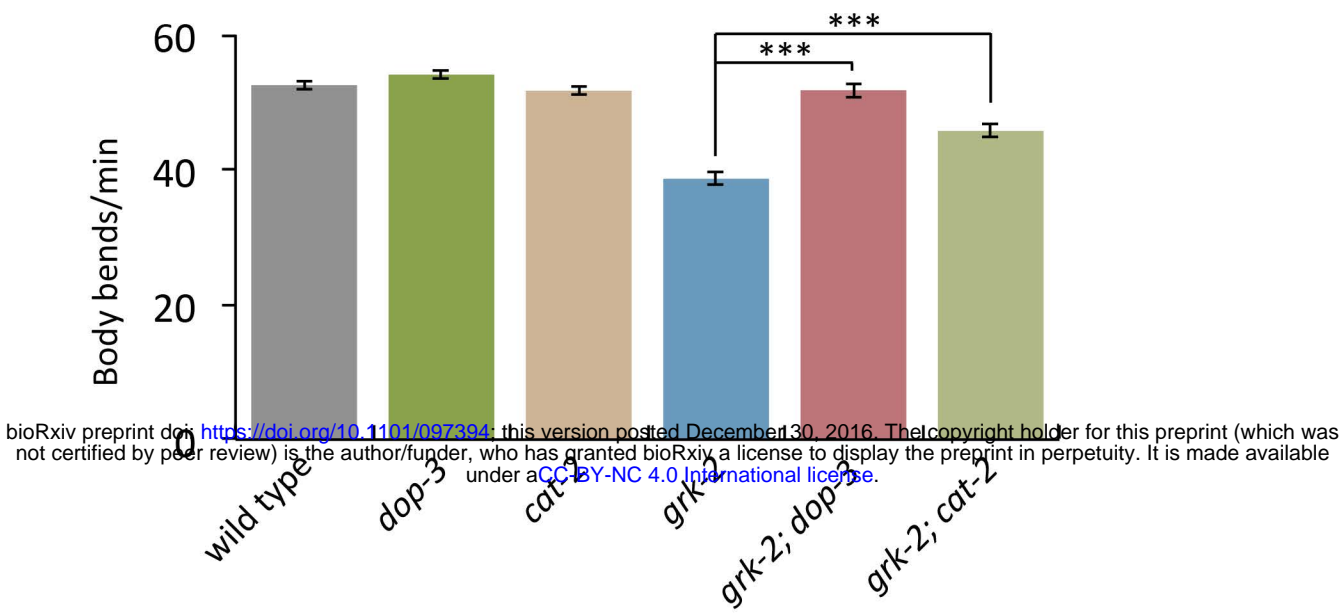
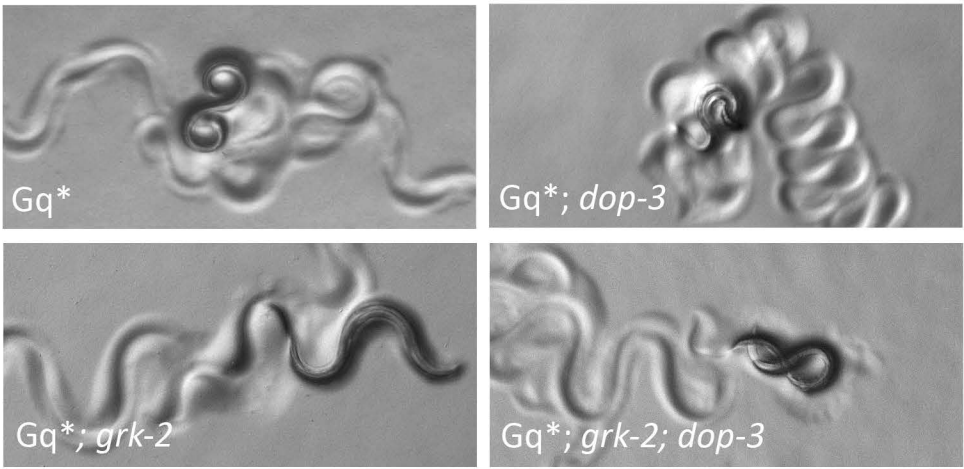


Fig 4

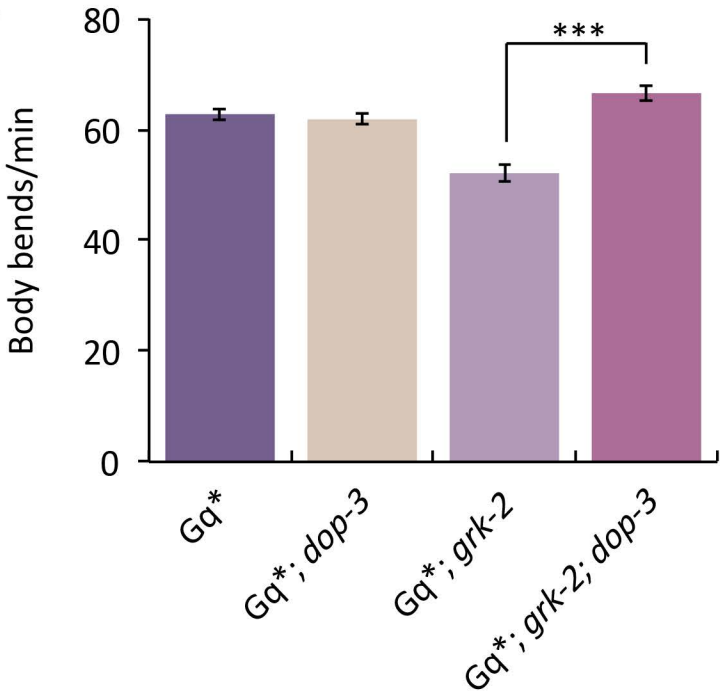
A



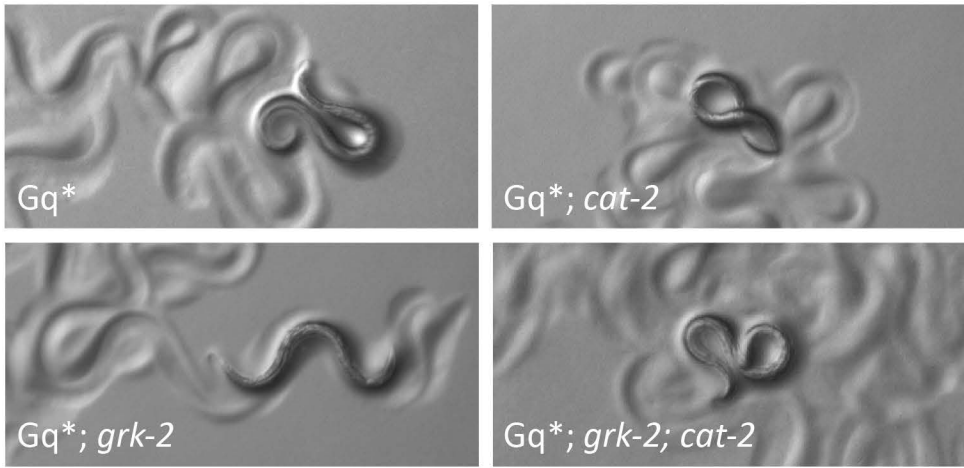
B



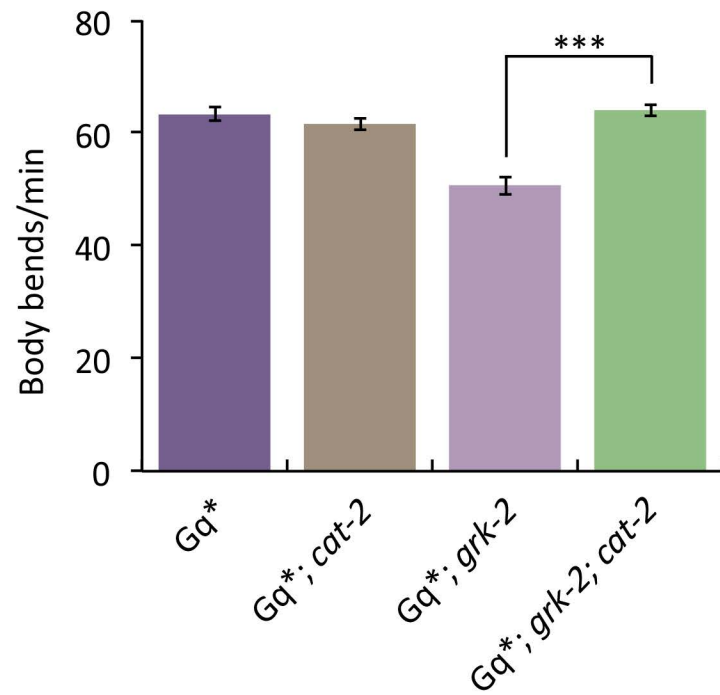
C



D



E



F

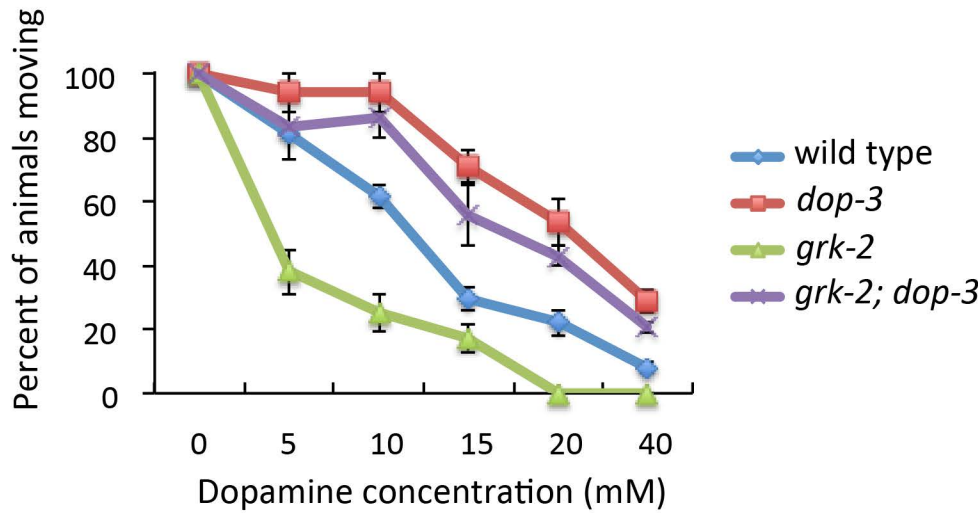
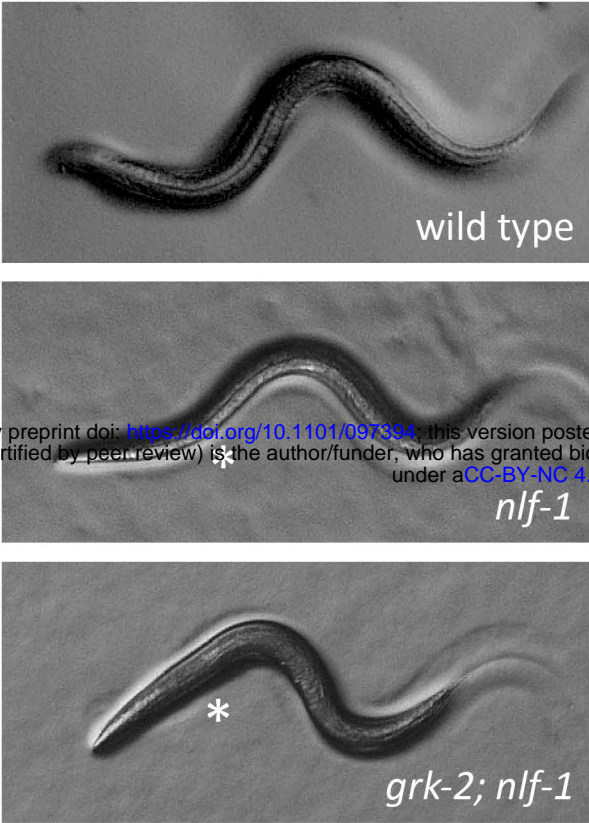
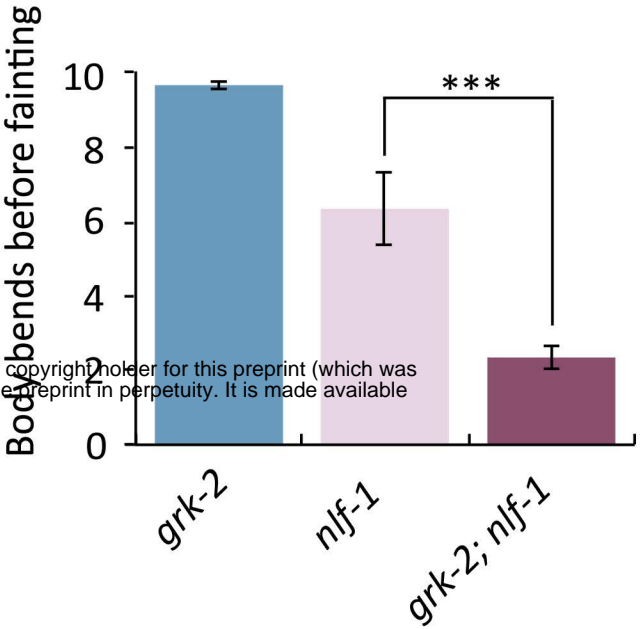


Fig 5

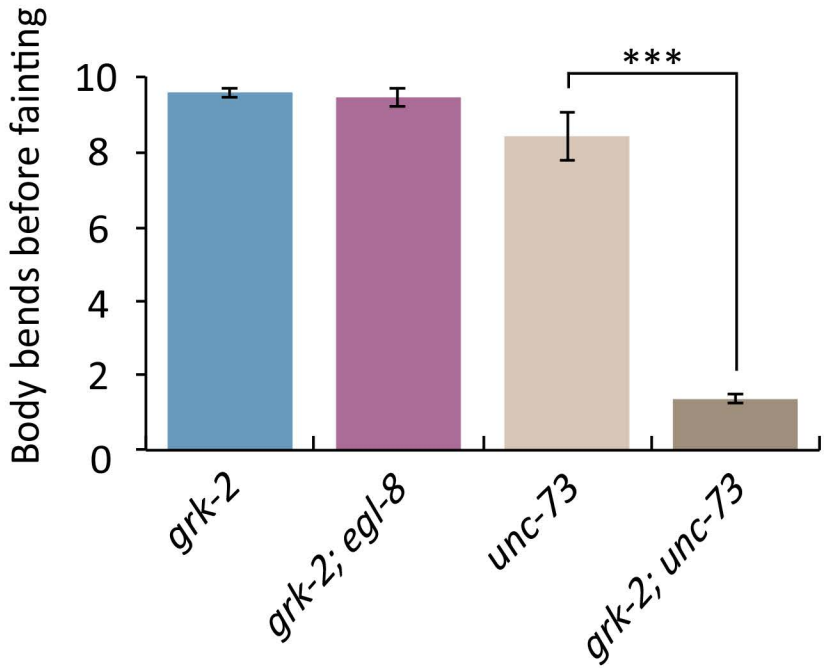
A



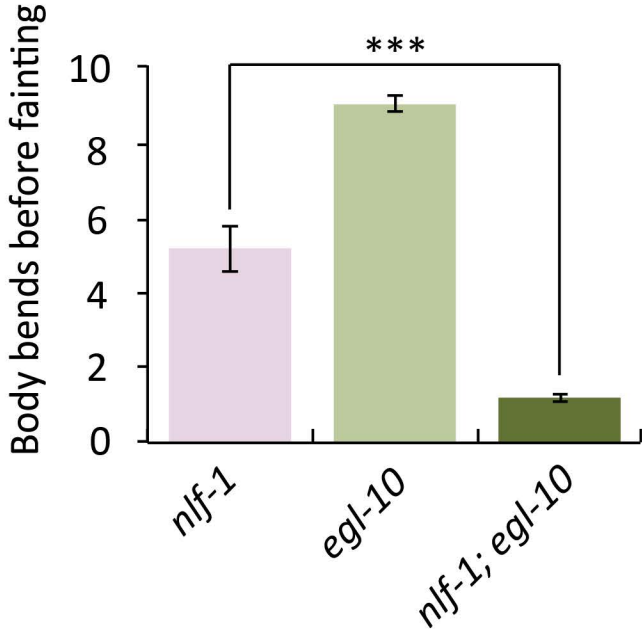
B



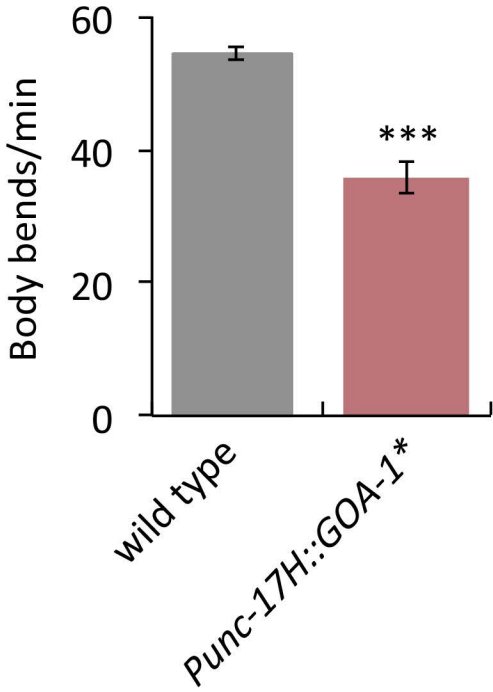
C



D



E



F

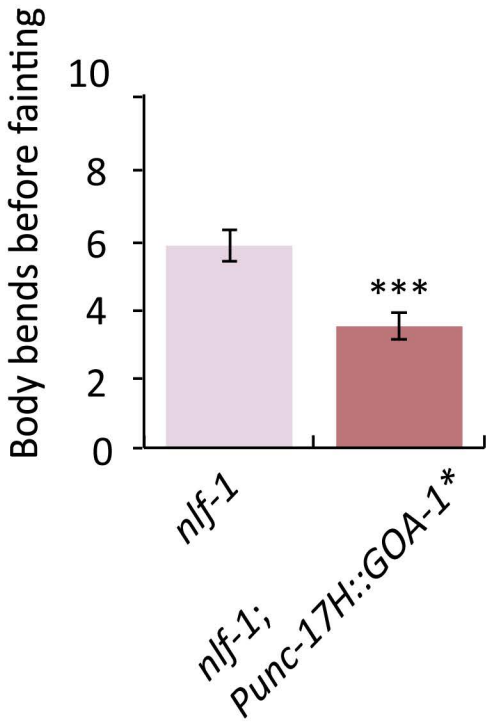
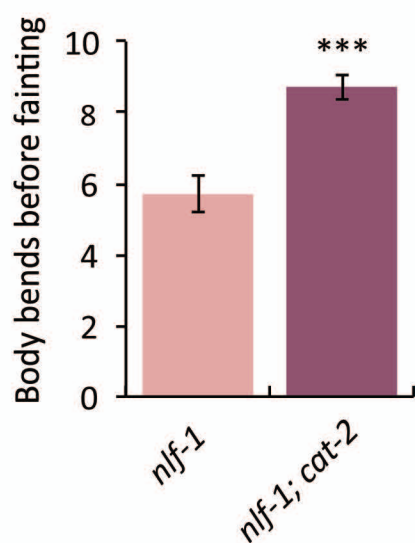
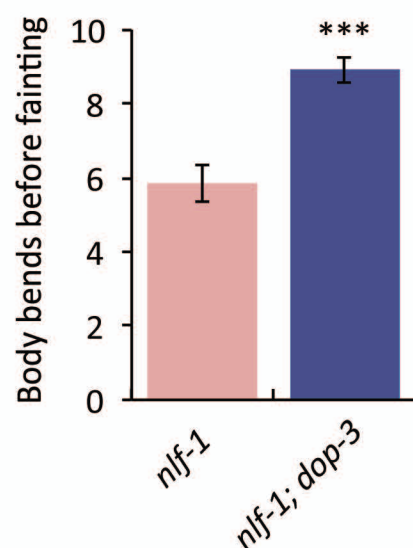


Fig 6

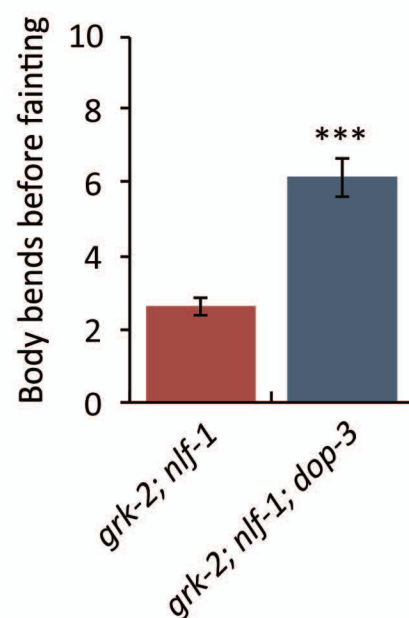
A



B



C



D

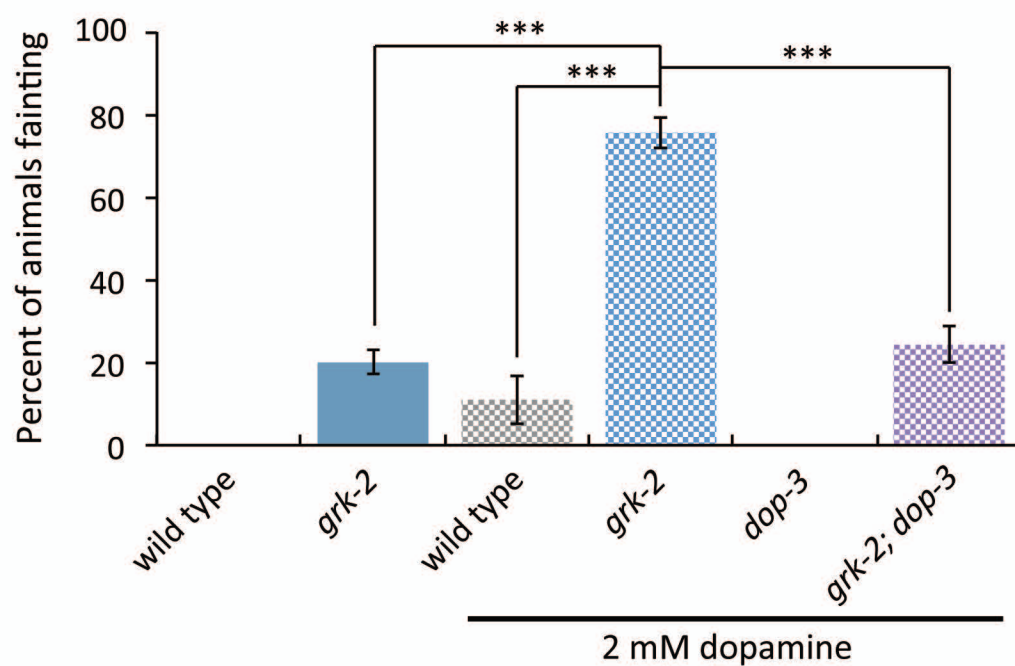
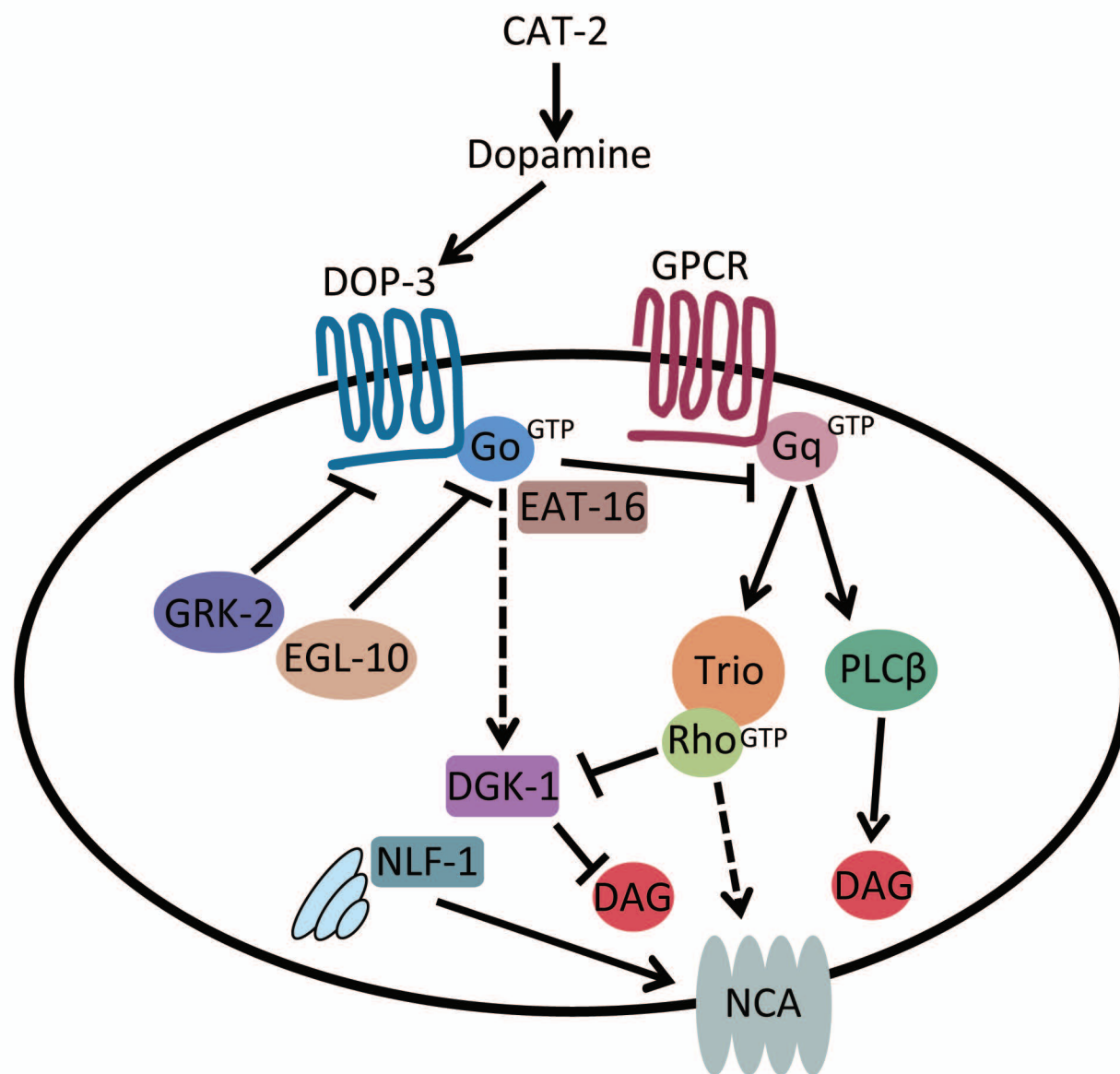
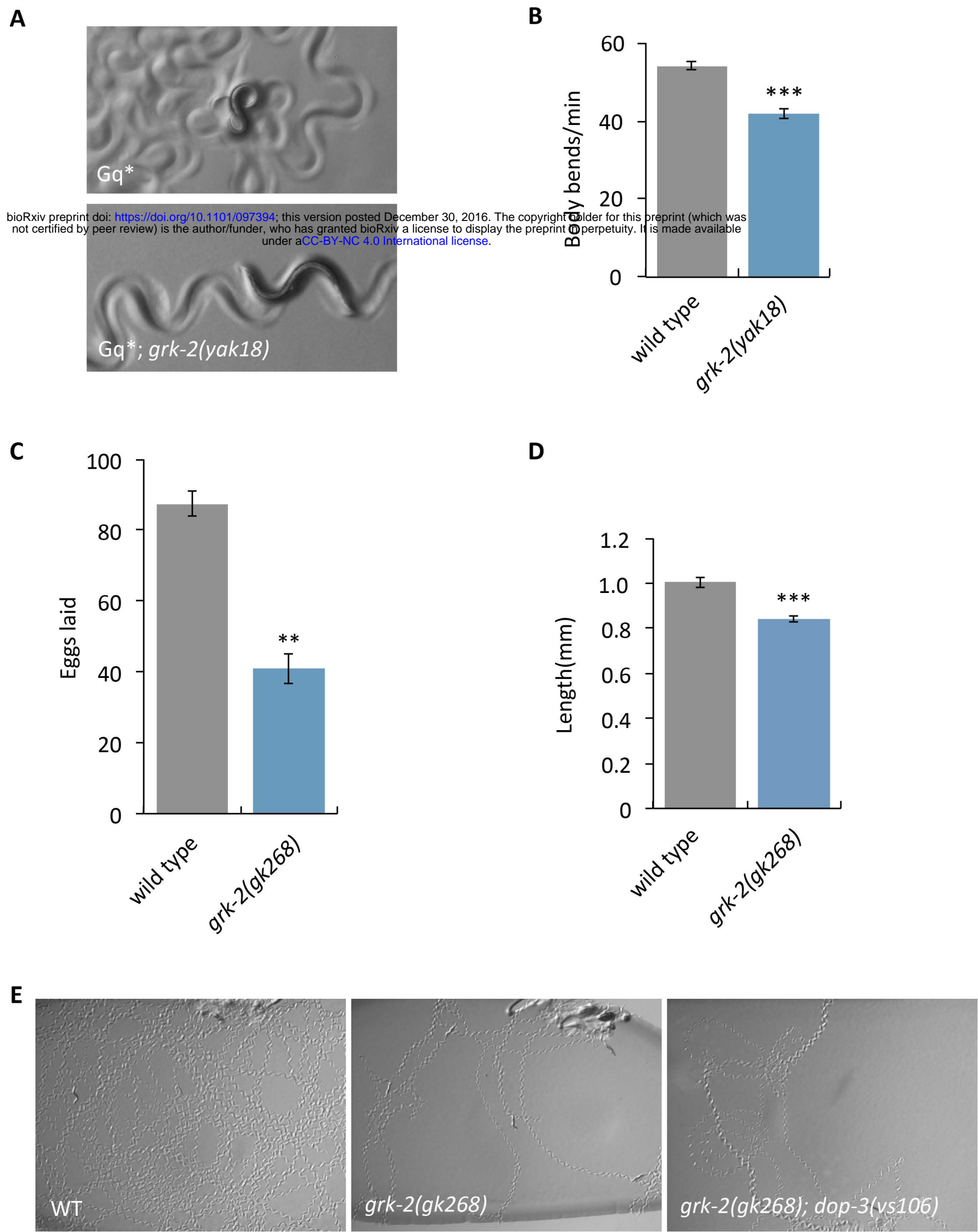


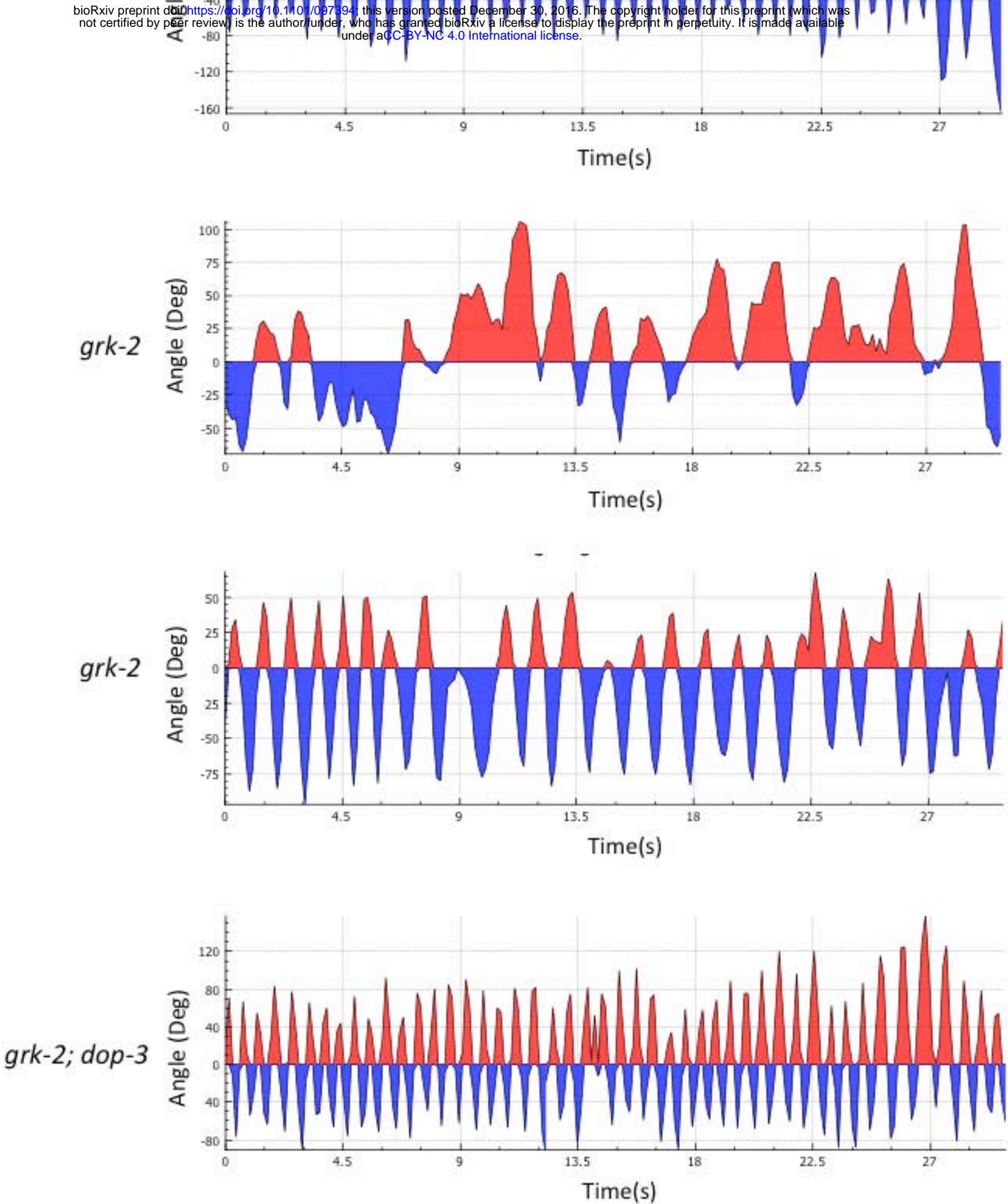
Fig 7



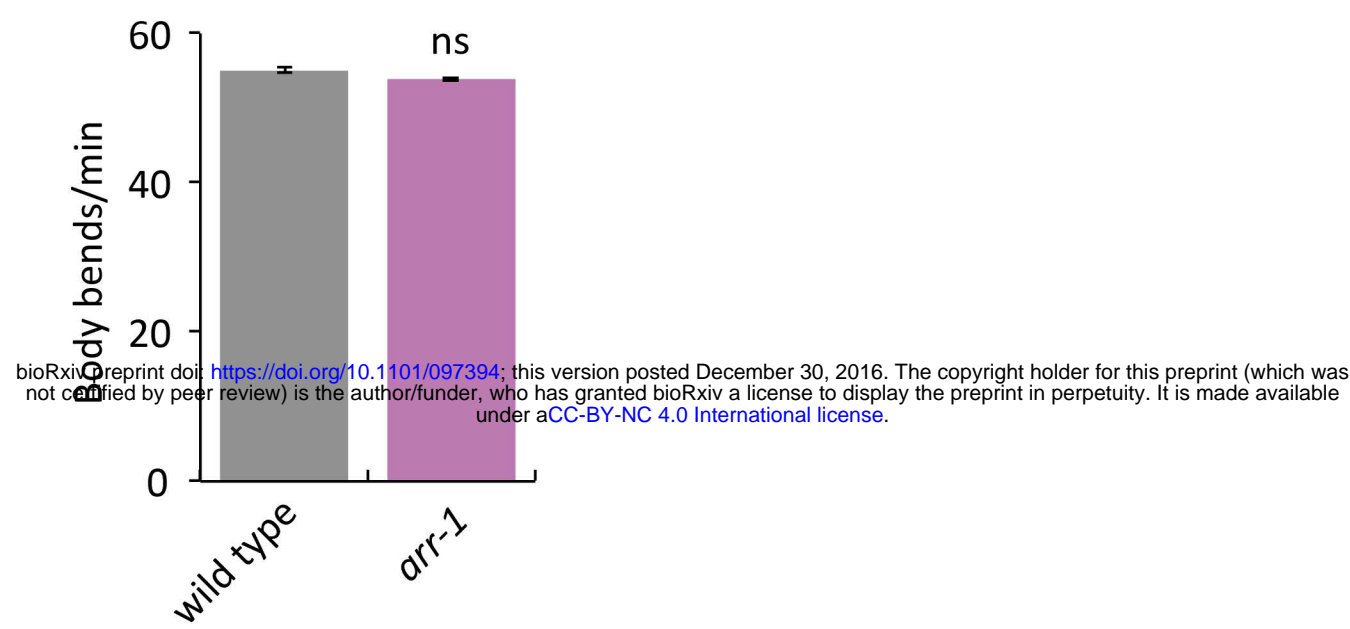
S1 Fig.



S2 Fig.

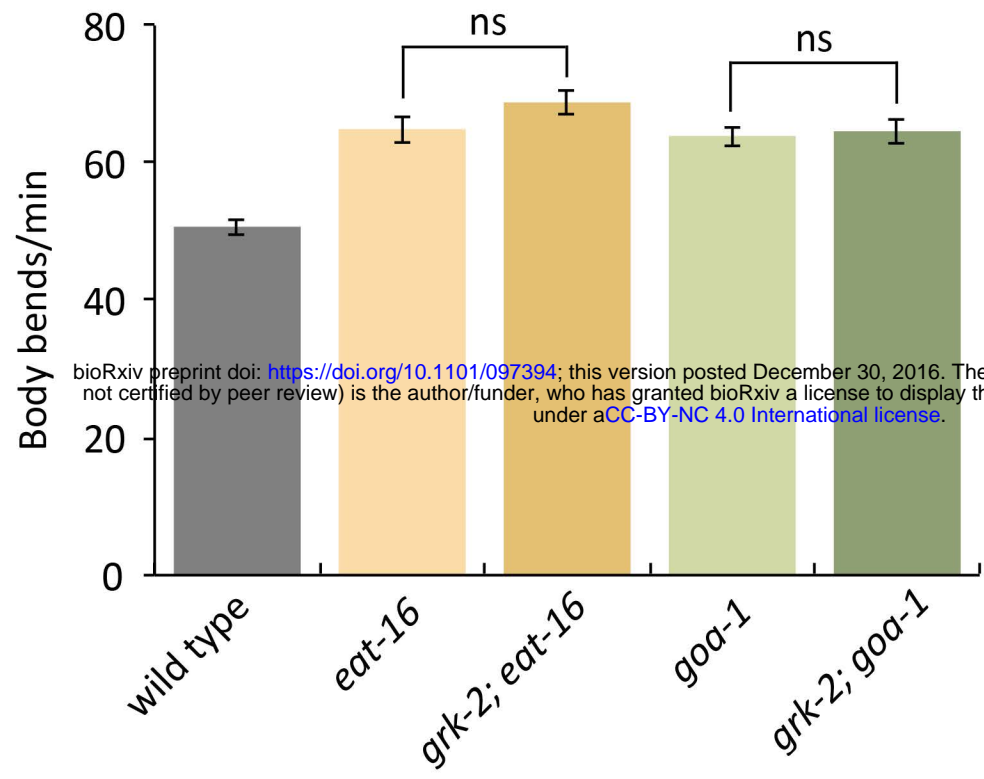


S3 Fig.

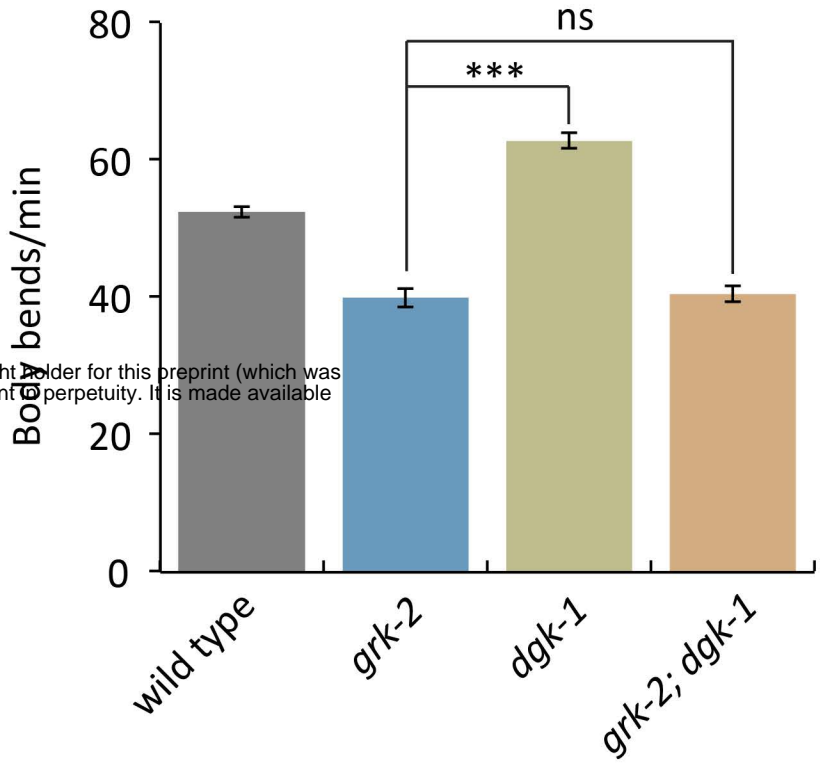


S4 Fig.

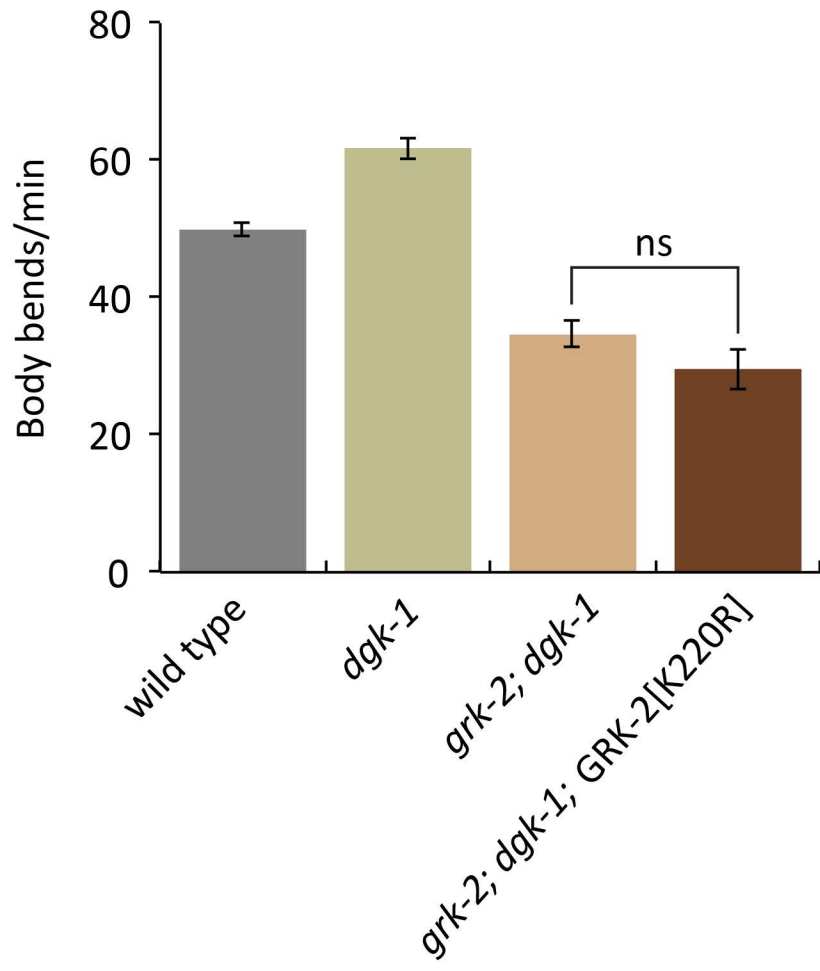
A



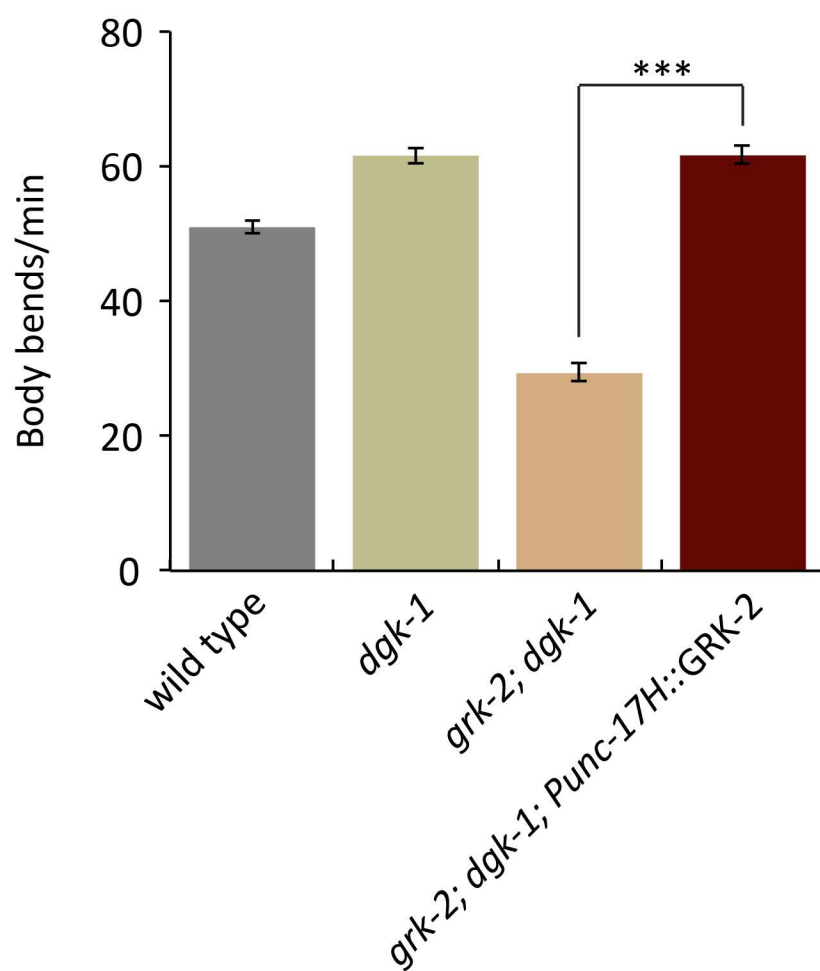
B



C

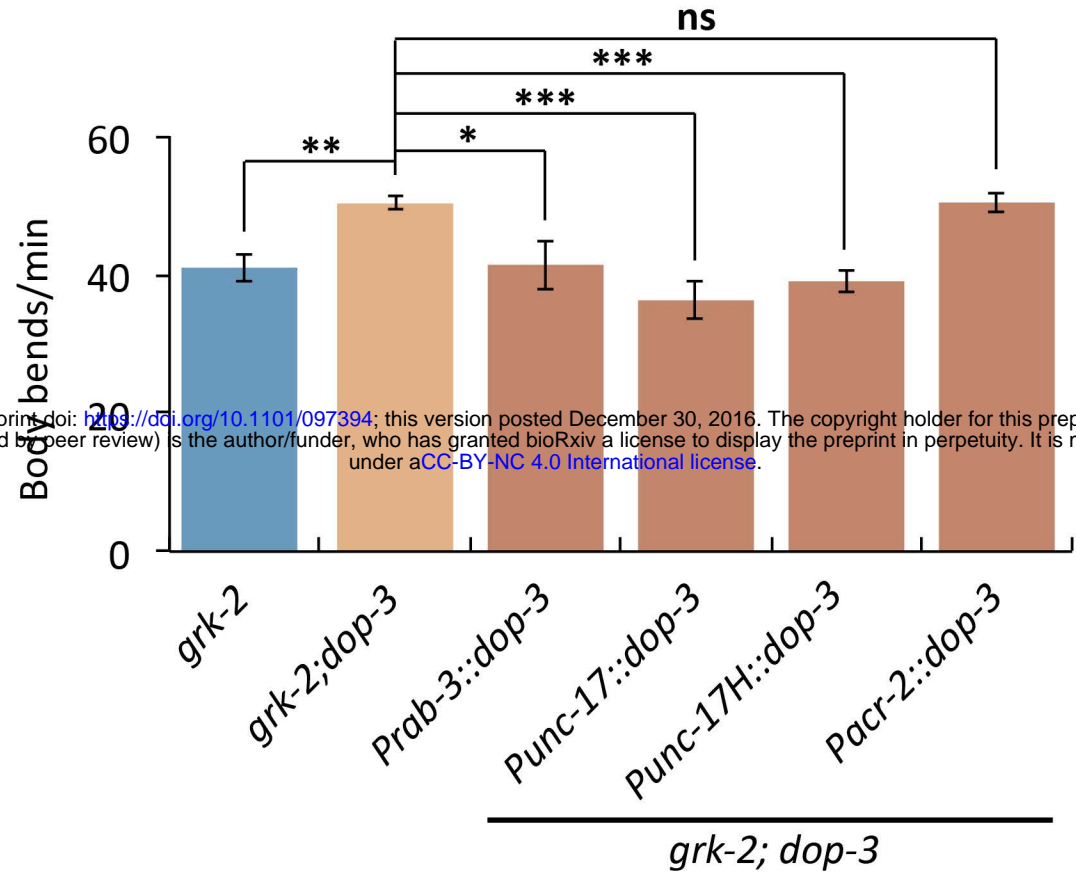


D

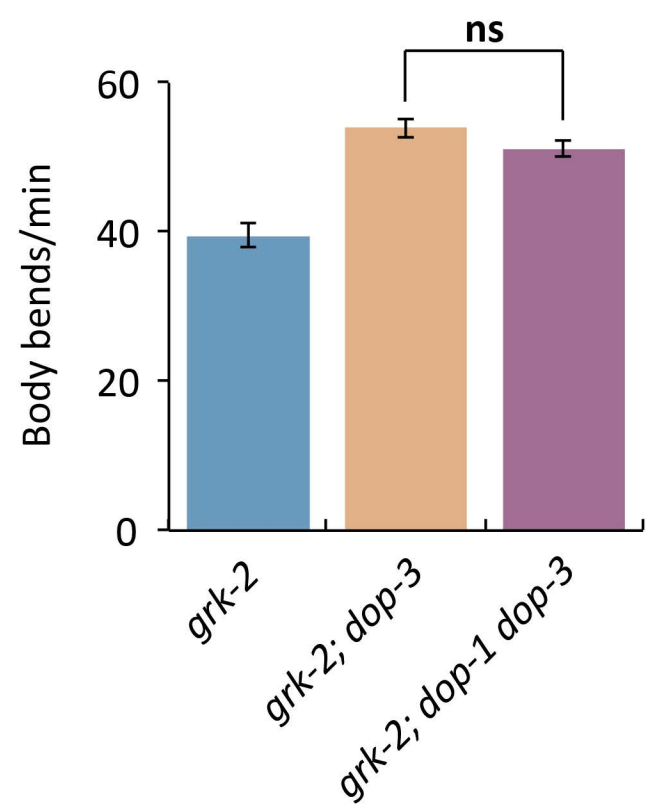


S5 Fig.

A

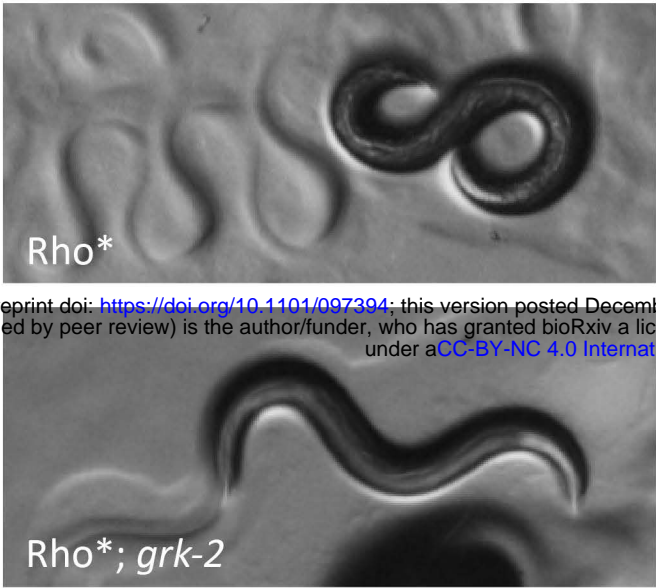


B



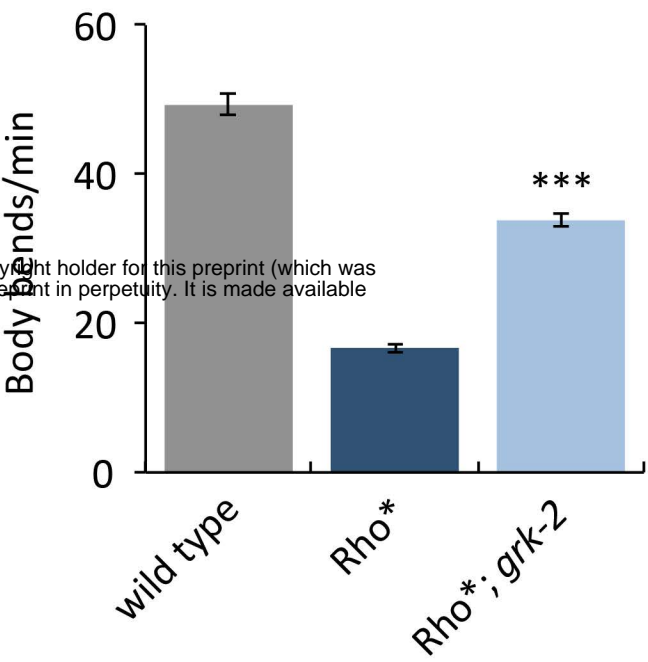
S6 Fig.

A

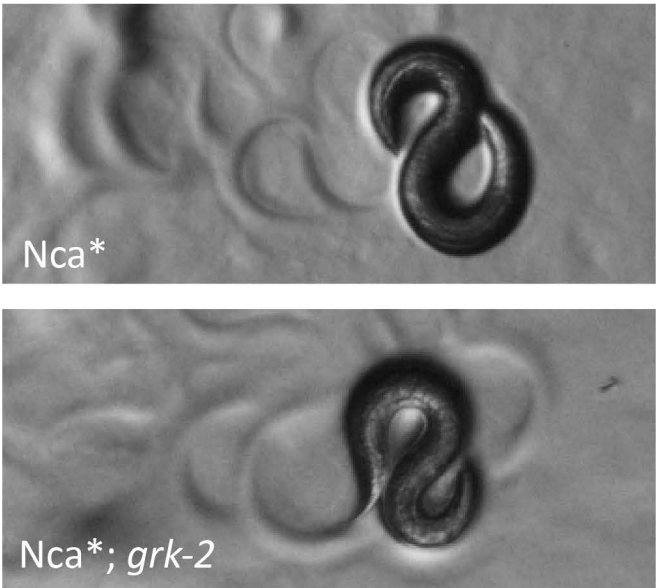


bioRxiv preprint doi: <https://doi.org/10.1101/097394>; this version posted December 30, 2016. The copyright holder for this preprint (which was not certified by peer review) is the author/funder, who has granted bioRxiv a license to display the preprint in perpetuity. It is made available under aCC-BY-NC 4.0 International license.

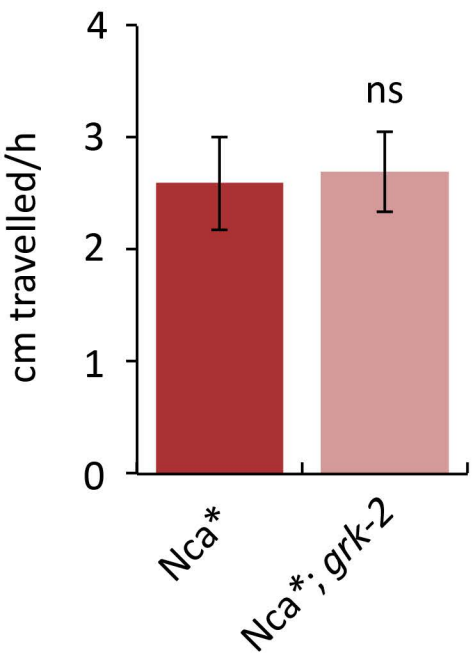
B



C

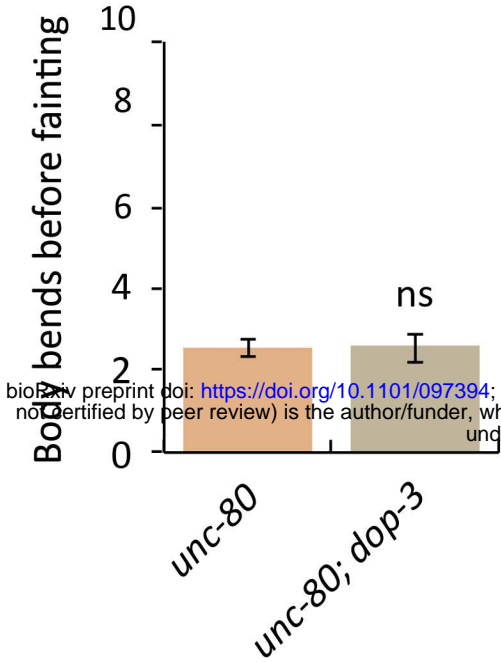


D

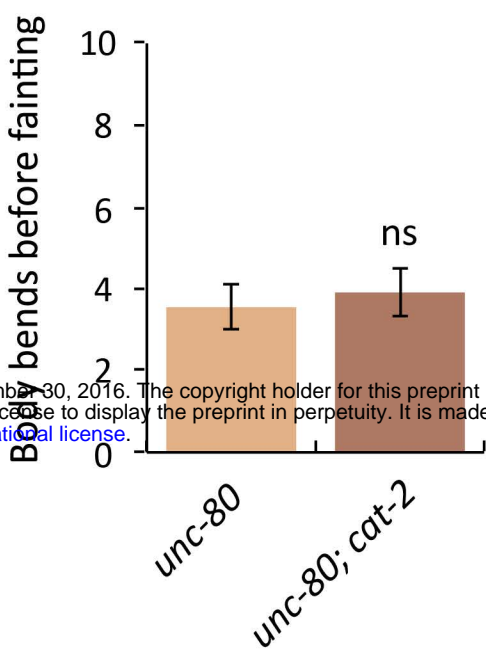


S7 Fig.

A



B



bioRxiv preprint doi: <https://doi.org/10.1101/097394>; this version posted December 30, 2016. The copyright holder for this preprint (which was not certified by peer review) is the author/funder, who has granted bioRxiv a license to display the preprint in perpetuity. It is made available under aCC-BY-NC 4.0 International license.

S1 Table. List of strains

N2: Bristol wild strain

CB1112: *cat-2(e1112)* II

CB4856: Hawaiian wild strain

EG317: *unc-73(ox317)* I

EG330: *unc-80(ox330)* V

EG352: *nca-1(ox352)* IV

EG4782: *nzIs29[Punc-17::rho-1(G14V), unc-122::gfp]* II

EG5504: *nlf-1(tm3631)* X

FG7: *grk-2(gk268)* III

JT47: *egl-8(sa47)* V

JT609: *eat-16(sa609)* I

JT734: *goa-1(sa734)* I

LX645: *dop-1(vs100)* X

LX703: *dop-3(vs106)* X

LX705: *dop-1(vs100)* X *dop-3(vs106)* X

MT8504: *egl-10(md176)* V

PS2627: *dgk-1(sy428)* X

RB660: *arr-1(ok401)* X

XZ1151: *egl-30(tg26)* I

The following strains were produced in this study:

XZ18: *grk-2(yak18)* III

XZ1089: *egl-30(tg26)* I ; *grk-2(yak18)* III

XZ1527: *egl-30(tg26)* I ; *grk-2(gk268)* III

XZ1531: *grk-2(gk268) III ; egl-8(sa47) V*

XZ1532: *unc-73(ox317) I ; grk-2(gk268) III*

XZ1544: *grk-2(gk268) III ; yakEx44[Prab-3::grk-2 cDNA::tbb-2 3'UTR::OPERON::GFP, Pmyo-3::mCherry]*

XZ1549: *grk-2(gk268) III ; yakEx45[Punc-17::grk-2 cDNA::tbb-2 3'UTR::OPERON::GFP, Pmyo-2::mCherry]*

XZ1551: *grk-2(gk268) III ; yakEx47[Pacr-2::grk-2 cDNA::tbb-2 3'UTR::OPERON::GFP, Pmyo-2::mCherry]*

XZ1552: *grk-2(gk268) III ; yakEx48[GRK-2[K220R], Pmyo-2::mCherry]*

XZ1559: *nzls29[Punc-17::rho-1(G14V), unc-122::gfp] II ; grk-2(gk268) III*

XZ1560: *grk-2(gk268) III ; nca-1(ox352) IV*

XZ1561: *grk-2(gk268) III ; yakEx51[Punc-17H::grk-2 cDNA::tbb-2 3'UTR::OPERON::GFP, Pmyo-3::mCherry]*

XZ1562: *grk-2(gk268) III ; yakEx52[Pglr-1::grk-2 cDNA::tbb-2 3'UTR::OPERON::GFP, Pmyo-2::mCherry]*

XZ1571: *grk-2(gk268) III ; yakEx54[Pgrk-2::grk-2 cDNA::tagRFP, Pmyo-3::GFP]*

XZ1579: *grk-2(gk268) III ; yakEx55[GRK-2[Y109I], Pmyo-2::mCherry]*

XZ1581: *grk-2(gk268) III ; dgk-1(sy428) X*

XZ1582: *grk-2(gk268) III ; yakEx57[GRK-2[R106A], Pmyo-2::mCherry]*

XZ1583: *grk-2(gk268) III ; yakEx56[GRK-2[D110A], Pmyo-2::mCherry]*

XZ1641: *grk-2(gk268) III ; yakEx71[Pxbx-1::grk-2 cDNA::tbb-2 3'UTR::OPERON_GFP, Pmyo-2::mCherry]*

XZ1675: *grk-2(gk268) III ; yakEx77[GRK-2[D3K], Pmyo-2::mCherry]*

XZ1676: *grk-2(gk268) III ; yakEx78[GRK-2[L4K], Pmyo-2::mCherry]*

XZ1684: *eat-16(sa609) I ; grk-2(gk268) III*

XZ1691: *nlf-1(tm3631) X ; grk-2(gk268) III*

XZ1692: *grk-2(gk268) III ; yakEx79[GRK-2[V7A/L8A], Pmyo-2::mCherry]*

XZ1693: *grk-2(gk268) III ; yakEx80[GRK-2[D10A], Pmyo-2::mCherry]*

XZ1694: *grk-2(gk268) III ; dgk-1(sy428) X ; yakEx51[Punc-17H::grk-2 cDNA::tbb-2 3'UTR::OPERON::GFP, Pmyo-3::mCherry]*

XZ1695: *grk-2(gk268) III ; dgk-1(sy428) X ; yakEx48[GRK-2[K220R], Pmyo-2::mCherry]*

XZ1713: *goa-1(sa734) I ; grk-2(gk268) III*

XZ1727: *grk-2(gk268) III ; yakEx87[GRK-2[K567E], Pmyo-2::mCherry]*

XZ1728: *grk-2(gk268) III ; yakEx88[GRK-2[R587Q], Pmyo-2::mCherry]*

XZ1766: *grk-2(gk268) III ; yakEx95[GRK-2[R195A], Pmyo-2::mCherry]*

XZ1767: *grk-2(gk268) III ; yakIs19[Pgrk-2::grk-2 cDNA::tagRFP] ; yakEx94[Punc-17H::eGFP::let-858 3'UTR]*

XZ1845: *yakEx103[Punc-17H::GOA-1[Q205L]::tbb-2 3'UTR::OPERON::GFP, Pmyo-2::mCherry]*

XZ1859: *egl-10(md176) V ; nlf-1(tm3631) X*

XZ1876: *nlf-1(tm3631) X ; yakEx103[Punc-17H::GOA-1[Q205L]::tbb-2 3'UTR::OPERON::GFP, Pmyo-2::mCherry]*

XZ1903: *grk-2(gk268) III ; dop-3(vs106) X*

XZ1904: *egl-30(tg26) I ; grk-2(gk268) III ; dop-3(vs106) X*

XZ1905: *cat-2(e1112) II ; grk-2(gk268) III*

XZ1906: *egl-30(tg26) I ; cat-2(e1112) II ; grk-2(gk268) III*

XZ1909: *grk-2(gk268) III ; dop-3(vs106) X ; yakEx109[Pacr-2::dop-3 cDNA::tbb-2 3'UTR::OPERON::GFP, Pmyo-2::mCherry]*

XZ1910: *grk-2(gk268) III ; dop-3(vs106) X ; yakEx110[Punc-17H::dop-3 cDNA::tbb-2 3'UTR::OPERON::GFP, Pmyo-2::mCherry]*

XZ1911: *grk-2(gk268) III ; dop-3(vs106) X ; yakEx111[Punc-17::dop-3 cDNA::tbb-2 3'UTR::OPERON::GFP, Pmyo-2::mCherry]*

XZ1912: *grk-2(gk268) III ; dop-3(vs106) X ; yakEx112[Prab-3::dop-3 cDNA::tbb-2 3'UTR::OPERON::GFP, Pmyo-2::mCherry]*

XZ1925: *cat-2(e1112) II ; unc-80(ox330) V*

XZ1935: *cat-2(e1112) II ; nlf-1(tm3631) X*

XZ1936: *unc-80(ox330) V ; dop-3(vs106) X*

XZ1940: *nlf-1(tm3631) X dop-3(vs106) X*

XZ1941: *grk-2(gk268) III ; nlf-1(tm3631) X dop-3(vs106) X*

XZ2007: *grk-2(gk268) III ; dop-1(vs100) X dop-3(vs106) X*

XZ2028: *egl-30(tg26) I ; grk-2(gk268) III ; yakEx48[GRK-2(K220R), Pmyo-2::mCherry]*

XZ2029: *egl-30(tg26) I ; grk-2(gk268) III ; yakEx51[Punc-17H::grk-2 cDNA::tbb-2*

3'UTR::OPERON::GFP, Pmyo-3::mCherry]

S2 Table. List of plasmids

Gateway destination vectors

pCFJ150 Gateway destination vector for insertion at chr II Mos site *ttTi5605*

Gateway entry clones

pADA180 *Punc-17H* [4-1] (head acetylcholine neurons)

p_C06E1.4_93 *Pglr-1* [4-1] (from Open Biosystems)

pCFJ31 *Pacr-2* [4-1]

pCFJ326 *tbb-2* 3'UTR::OPERON::GFP [2-3]

pCR185 GFP::*unc-54* 3'UTR [2-3]

pEGB05 *Prab-3* [4-1]

pET68 *grk-2* cDNA [1-2]

pET89 *Pgrk-2* [4-1]

pET108 *Pxbx-1* [4-1] (425bp promoter sequence upstream of the ATG)

pET134 *goa-1*[Q205L] cDNA [1-2]

pET139 *dop-3* cDNA [1-2]

pGH1 *Punc-17* [4-1]

pGH107 tagRFP::*let-858* 3'UTR [2-3]

Gateway expression constructs

pET79 *Prab-3*::*grk-2* cDNA:*tbb-2* 3'UTR::OPERON::GFP_pCFJ150

pET81 *Punc-17*::*grk-2* cDNA::*tbb-2* 3'UTR::OPERON::GFP_pCFJ150

pET82	<i>Punc-17H::grk-2 cDNA::tbb-2 3'UTR::OPERON::GFP_pCFJ150</i>
pET83	<i>Pacr-2::grk-2 cDNA::tbb-2 3'UTR::OPERON::GFP_pCFJ150</i>
pET88	<i>Pglr-1::grk-2 cDNA::tbb-2 3'UTR::OPERON::GFP_pCFJ150</i>
pET90	<i>Pgrk-2::grk-2 cDNA::GFP_pCFJ150</i>
pET91	<i>Pgrk-2::grk-2 cDNA::tagRFP_pCFJ150</i>
pET93	<i>Punc-17H::eGFP::let-858 3'UTR_pCFJ150</i>
pET109	<i>Pxbx-1::grk-2 cDNA::tbb-2 3'UTR::OPERON::GFP_pCFJ150</i>
pET135	<i>Punc-17H::GOA-1[Q205L]::tbb-2 3'UTR::OPERON::GFP_pCFJ150</i>
pET140	<i>Prab-3::dop-3 cDNA::tbb-2 3'UTR::OPERON::GFP_pCFJ150</i>
pET141	<i>Pacr-2::dop-3 cDNA::tbb-2 3'UTR::OPERON::GFP_pCFJ150</i>
pET142	<i>Punc-17::dop-3 cDNA::tbb-2 3'UTR::OPERON::GFP_pCFJ150</i>
pET143	<i>Punc-17H::dop-3 cDNA::tbb-2 3'UTR::OPERON::GFP_pCFJ150</i>

Plasmids used for the GRK-2 structure-function analysis: from Wood et al., 2012.

pFG45	<i>Pgrk-2::GRK-2</i>
pFG46	<i>Pgrk-2::GRK-2[D3K]</i>
pFG47	<i>Pgrk-2::GRK-2[L4K]</i>
pFG48	<i>Pgrk-2::GRK-2[V7A/L8A]</i>
pFG49	<i>Pgrk-2::GRK-2[D10A]</i>
pFG84	<i>Pgrk-2::GRK-2[R195A]</i>
pFG85	<i>Pgrk-2::GRK-2[R106A]</i>
pFG86	<i>Pgrk-2::GRK-2[Y109I]</i>

pFG87	<i>Pgrk-2::GRK-2</i> [D110A]
pFG88	<i>Pgrk-2::GRK-2</i> [K220R]
pFG89	<i>Pgrk-2::GRK-2</i> [K567E]
pFG90	<i>Pgrk-2::GRK-2</i> [R587Q]